

NORTHWESTERN UNIVERSITY

Synchronization in Visual Attention and Binocular Rivalry

A DISSERTATION

SUBMITTED TO THE GRADUATE SCHOOL IN PARTIAL FULFILLMENT OF THE  
REQUIREMENTS

for the degree

DOCTOR OF PHILOSOPHY

Field of Psychology

By

Yee Joon Kim

EVANSTON, ILLINOIS

June 2008

**ABSTRACT**

## Synchronization in Visual Attention and Binocular Rivalry

Yee Joon Kim

The human brain shows great flexibility to adjust itself to dynamically ever-changing environment. Despite more than 100 years of cognitive brain research, the dynamical aspect of cognitive process has remained poorly understood compared to the static aspect of that.

This dissertation concerns the dynamic character and functional significance of periodically forced synchronization in visual attention and binocular rivalry. The hypotheses, experimental paradigms, data analyses, and interpretation of the results were inspired by recent insights from physics and neuroscience – most notable the theory of synchronization and the phenomenon of stochastic resonance whose applicability to cognitive processes is explained.

In the first and the second electroencephalography (EEG) experiment, we show that voluntary sustained visual attention multiplicatively increases the stimulus-location selective population electrophysiological activity by monitoring frequency-tagged steady-state visual evoked potentials (SSVEP) in human brain. Furthermore, analyses of inter-trial phase coherence show that this attentional response gain is at least partially due to increased synchronization of SSVEPs to stimulus flicker. Finally, it is revealed that the harmonic-based topographic difference exists in that the scalp distribution of the fundamental harmonic is central/bilateral and that of the second harmonic is contralateral. In the third behavioral experiment, we demonstrate quantitative evidence of stochastic resonance in binocular rivalry by subjecting binocular rivalry to weak periodic contrast modulations spanning a range of frequencies.

We propose that the experimental findings in the frequency-locked SSVEP activities – the multiplicative response gain in SSVEPs by sustained visual attention, the harmonic-dependent topographic differences – and the stochastic resonance in binocular rivalry may find a unifying explanation within the theory of synchronization. This theory offers a general mechanism for the emergence of collective dynamics in large networks with many units adjusting a given property of their motion due to a suitable coupling configuration, or to an external forcing.

Based on the above results, we conjecture that a mechanism of synchronization in nonlinear dynamical systems may be a general organizing principle of great importance for cognitive processes and account for how we perceive and react to the outside world.

Thank you for My Glorious Leaders, Satoru, Marcia, and Ken.

그리고 멀리서 항상 응원해주신 우리 아버님 가피력에도

감사드립니다.

## TABLE OF CONTENTS

CHAPTER	Page
1 INTRODUCTION .....	9
Overview.....	9
Outline.....	9
2 THEORY OF SYNCHRONIZATION AND THE BRAIN .....	10
The basic notions in synchronization.....	10
Forms of synchronization .....	11
Forced synchronization.....	13
Mutual synchronization .....	14
Stochastic resonance / Stochastic synchronization .....	15
The application of synchronization ideas to cognitive processes .....	17
3 SYNCHRONIZATION AT ELECTROPHYSIOLOGICAL LEVEL .....	18
Experiment 1 – Attention induces synchronization-based response gain in steady-state visual evoked potentials .....	18
Introduction.....	18
Procedure .....	24
Results.....	29
Discussion.....	32
Experiment 2 – Parallel visual processing revealed by evoked oscillatory neural harmonics .....	38
Introduction.....	39
Procedure .....	42

CHAPTER	Page
Results.....	45
Discussion.....	49
4 SYNCHRONIZATION AT BEHAVIORAL LEVEL	
Experiment 3 – Stochastic resonance in binocular rivalry .....	51
Introduction.....	51
Procedure .....	60
Results.....	63
Discussion.....	67
5 CONCLUSION .....	78
REFERENCES .....	80
FIGURES.....	89

## LIST OF FIGURES

FIGURE	Page
1	Motion of a particle in a double-well potential.....89
1-1	The contrast-, response-, and activity-gain hypotheses regarding how voluntary visual spatial attention boosts neural responses.....89
1-2	Stimuli and a trial sequence .....90
1-3	Topographic plots of 2 <sup>nd</sup> harmonic of the standardized SSVEPs .....91
1-4	SSVEP contrast-response functions.....92
1-5	Representative simulation results .....93
1-6	ITPC for second-harmonic SSVEPs .....94
1-7	Contrast dependence of inter-trial phase coherence (ITPC) for SSVEPs.....95
1-8	Examples of probe displays for the control experiment .....96
2-1	Stimuli and a trial sequence .....97
2-2	Topographic difference between the 1 <sup>st</sup> and 2 <sup>nd</sup> harmonic of the standardized SSVEPs.....97
2-3	Stimuli and a trial sequence .....99
2-4	Attentional modulation of the 1 <sup>st</sup> and 2 <sup>nd</sup> harmonic.....99
3-1	A cartoon illustration of a double-well potential framework describing binocular rivalry under periodic contrast modulations .....101
3-2	The stimuli used to induce binocular rivalry .....101
3-3	Distributions of perceptual dominance duration in binocular rivalry .....102
3-4	P <sub>1</sub> amplitude and gain due to periodic contrast-modulation signals.....103

FIGURE

3-5 Coefficient of variation (CV = standard deviation/mean) as a function of the contrast-modulation frequency (Hz).....104

3-6 The relationship between the resonance frequency (the contrast-modulation frequency that minimizes CV) and the mean spontaneous alternation rate.....104

3-7 Fitting the dominance-duration distributions for contrast-modulation frequencies from 0.28 to 2.48 Hz (with the corresponding half-periods [HP] from 1800 to 200 ms), using the astable multivibrator model based on a Schmitt trigger (known to exhibit stochastic resonance) .....105

## **Synchronization in Visual Attention and Binocular Rivalry**

### **1. INTRODUCTION**

This dissertation concerns the nature of stimulus-induced synchronization in visual spatial attention and binocular rivalry. Especially the idea of forced synchronization by external periodic signals will be applied to the cognitive processes. The cognitive processes will be subjected to the dynamic sensory input to investigate how it can modulate or induce population electrophysiological activity and behavioral activity during the cognitive processes. The most fundamental prediction of the synchronization theory is an entrainment of temporal dynamics of these cognitive processes, which should be reflected in the *frequency entrainment* (time-scale matching) between the external periodic signal and the stimulus-induced activity in the brain. We further hypothesized that sustained voluntary visual attention increase the phase-locked electrophysiological activity to the external stimulus dynamics. The interaction between external signal and stimulus-induced activities is also hypothesized to give rise to stochastic resonance in perception and behavior.

To summarize in neuroscientific terms, the aim of this dissertation is to characterize the state of the brain during sustained visual attention and binocular rivalry, as indexed by synchronized activity, and how this state is affected by and affects the processing of incoming information from our dynamic sensory environment.

#### *Outline*

Throughout this dissertation, I treat the relevance and limitations of certain theoretical frameworks of synchronization in nonlinear dynamical systems to three current experimental studies (Experiment 1- Experiment 3) that were taken in this thesis and review the main results of the studies.

Chapter 2 briefly reviews the theory of synchronization that is relevant to our current studies and discusses the applicability of synchronization ideas to cognitive processes to further understanding of the state of the human brain during processing incoming information from our dynamic sensory environment. The main aims, the general procedures, the main results, and the discussions of three experimental studies are described in Chapter 3 and 4, respectively. The main conclusion is found in Chapter 5.

## **2. THEORY OF SYNCHRONIZATION AND THE BRAIN**

To appreciate the functional significance of synchronization in human brain function, it is instructive to specify the basic notions in the theory of synchronization and list several different forms of synchronization relevant to our current experiments. Finally the applicability of synchronization ideas to human brain functions, particularly cognitive processes, is discussed.

### *The basic notions in synchronization*

Synchronization is a process where oscillating objects adjust their rhythms due to their interaction. In physics such oscillatory objects are meant by *self-sustained oscillators*. The main universal property of self-sustained oscillators is that they are active systems that are capable of generating their own rhythms even if they are isolated. This continuous oscillation is maintained by an internal source of energy until it dissipates in the system. When this oscillation is perturbed, the oscillation soon returns to its original shape. Mathematically, these oscillators are called *autonomous* (i.e. without explicit time dependence). Many natural systems such as single cells that fire action potentials, cardiac pacemakers that control human heartbeat, a firefly that emits light pulse, and biological clocks that generate circadian rhythms, etc. are considered as self-sustained systems. Only these kinds of systems have the ability to be synchronized.

Now we briefly summarize the key notions of synchronization of self-sustained oscillators.

*Frequency locking* (or *entrainment*) is a phenomenon where nonidentical oscillators having their own frequencies when coupled together adjust their rhythms and start to oscillate with a common frequency.

*Coupling strength* describes how weak (or how strong) the interaction among oscillators is. In an experimental situation it is not always clear how to measure this quantity. If oscillators do not interact, the coupling strength is zero. If coupling is too strong, that makes the whole system of oscillators unified.

*Frequency mismatch* (or *detuning*) quantifies how different the uncoupled oscillators are. Synchronization takes place if the mismatch of uncoupled systems is not very large.

*Phase locking* is a certain relationship between the phases of synchronized self-sustained oscillators. It means that the phase difference is constant when oscillators are synchronized.

Based upon the above notions synchronization can be redefined as a phenomenon where nonidentical oscillators with initially different frequencies and independent phases adjust their rhythms and start to oscillate with a common frequency (*frequency locking*) when they are coupled together; this also implies a definite relation between the phases of systems (*phase locking*). The adjustment of rhythms occurs in a certain range of systems' mismatch; in particular, if the frequency of one oscillator is slowly varied, the rest of the system follows this variation.

### *Forms of synchronization*

There are numerous ways to affect oscillators. There is no standardized taxonomy of the mechanisms that modify oscillators. The forms of synchronization are usually classified by

paying more attention to certain general properties, e.g., whether the oscillations are periodic or irregular, or whether the coupling is unidirectional or bidirectional. A variety of synchronization phenomena, first discovered by Christiaan Huygens in the 17<sup>th</sup> century (Huygens, 1673), have been investigated in periodic, chaotic, and stochastic systems.

In periodic system, there are two classical types of synchronization in general – a *forced synchronization*, i.e., the synchronization of oscillations by an external periodic signal, and a *mutual synchronization*, which is observed under the interaction of more than two self-oscillating systems. These two classical phenomena are characterized by the locking of natural frequencies (and, consequently, phases) of oscillations or the suppression of one of the two frequencies of quasiperiodic oscillations.

In chaotic systems, many different kinds of synchronization phenomena take place, from complete synchronization (Fujisaka & Yamada, 1983), to phase (Rosenblum *et al.*, 1996) and lag synchronization (Rosenblum *et al.*, 1997), generalized synchronization (Rulkov *et al.*, 1995), intermittent lag synchronization (Rosenblum *et al.*, 1997), imperfect phase synchronization (Zaks *et al.*, 1999), and almost synchronization (Femat & Solis-Perales, 1999).

In stochastic systems, stochastic synchronization known as *stochastic resonance* has been observed in the systems with noise-induced switching (Gammaitoni *et al.*, 1998). While noise is normally considered harmful to the optimal performance in many systems, in stochastic resonance, optimal noise added to nonlinear noise-induced oscillatory system improves its sensitivity to weak coherent signals. As one might expect, the amount of noise in stochastic resonance is critical for the proper amplification of the external weak coherent signal: too much noise increasingly corrupts the signal, whereas the signal does not get through when too little noise exists. This noise-based optimization is the essence of stochastic resonance. Thus,

stochastic resonance gives us a rare chance to see the nature of noise that is added to the external signal externally or internally by the system.

Here we will look further at two classical types of synchronization (e.g. forced synchronization and mutual synchronization) and stochastic resonance for later application to three experimental studies.

### *Forced synchronization*

This entrainment of a self-sustained oscillator by an external periodic force is the classical example of synchronization. Here the form of the periodic forcing can be harmonic, rectangular, or pulse-like. Probably the well-known examples of a living nature are the biological clocks that control the circadian rhythms of cells and the organisms controlled by the periodic rhythms originating from the rotation of the Earth around its axis and around the Sun. Obviously, the action here is unidirectional.

From the mathematical point of view, the theory of phase synchronization of periodic self-sustained oscillators is well established (Andronov, 1966; Anishchenko *et al*, 2003; Hayashi, 1964; Guckenheimer & Holmes, 1983, Pikovsky *et al*, 2003). If  $\Phi(t)$  is the phase of a periodic oscillator and  $\Psi(t)$  is the phase of an external periodic force, then the condition of synchronization can be formulated as

$$|m\Phi(t) - n\Psi(t)| = \text{const.}, \quad (1)$$

where  $m$  and  $n$  are integers. This condition defines the locking of two phases  $\Phi(t)$  and  $\Psi(t)$  and requires that the phase difference should be constant. Synchronization is also defined as frequency entrainment, provided that the frequencies of the oscillator and the driving force are in rational relation. Mostly the simplest case of 1:1 synchronization is considered. But

synchronization may occur in a more complicated form as long as the *Poincaré rotation number*, the ratio of frequencies  $\theta = \omega_1 / \omega$ , satisfies rational relation. Here,  $\omega_1$  is the driving frequency and  $\omega$  is the frequency of the oscillator. In case of the synchronization at the fundamental mode, we have  $\omega = \omega_1$ , and  $\theta$  is equal to unity. When  $\theta = m : n$ , as  $\omega_1$  varies, the frequency  $\omega$  will follow the driving frequency so that their ratio remains fixed in a certain finite range of parameters of the system, called the *domain of synchronization*. In this case we call this synchronization of higher order as *synchronization of the order  $m : n$* . Generally, synchronization of order  $m : n$  can be observed in experiment. For large  $m$  and  $n$  the synchronization domains are very narrow so that it is not always possible to observe them experimentally.

#### *Mutual synchronization*

In contrast to forced synchronization the coupling in mutual synchronization is bidirectional. This mutual synchronization involves the interactions of more than two oscillating objects with different natural frequencies. They equally affect each other and mutually adjust their rhythms. The most spectacular example of mutual synchronization in nature is a large population of fireflies flashing in synchrony. This type of synchronization occurs in many other populations of biological oscillators such as the pacemaker cells of heart, networks of neurons in the circadian pacemaker and hippocampus, the insulin-secreting cells of the pancreas, crickets that chirp in unison, groups of women whose menstrual periods become mutually synchronized (Strogatz, 2003).

The effect of mutually coupled oscillators is very similar to the case of external forcing. Both the forced and mutual synchronizations have a constant and rational value of the Poincaré rotation number  $\theta = m : n$ , which is preserved in the synchronization domain. Also the phase locking in mutual synchronization satisfies Eq. (1).

But there are some specific features in mutually coupled systems. One of the interesting features in these systems is the formation of synchronous *clusters*. Suppose the oscillators have slightly different frequencies that are somehow distributed over the ensemble of oscillators. If the interaction is very weak, there will be no synchronization so that all the systems will oscillate with their own frequencies. Also if the coupling is sufficiently strong, it can synchronize the whole ensemble, provided the natural frequencies are not too different. For an intermediate coupling or a broader distribution of natural frequencies of elements some partially synchronous states can be expected. In this way several oscillators synchronize and oscillate with a common frequency, whereas their neighbors have their own different frequencies. This is how clusters of synchronized elements appear.

In neuroscience literature this type of synchronization in large ensembles of neurons has been related to several central issues of neuroscience (Gray *et al.*, 1989; Singer & Gray, 1995; Singer, 1999; Varela *et al.*, 2001; Ward, 2003). Synchronization seems to be a central mechanism for neuronal information processing within a brain area as well as for communication among different brain areas. Their important message is that representation of the various attributes of the visual world by distributed neuronal assemblies can be bound together harmoniously in the time domain through oscillatory synchrony.

#### *Stochastic resonance / Stochastic synchronization*

There exist examples of systems in nature in which oscillations arise only under the influence of noise. Here we will discuss *noise-induced oscillations* excited by rapidly fluctuating forces. Unlike any other dynamical systems here the noise plays a crucial role in the dynamics: without fluctuations there are no oscillations at all. Because such systems oscillate without external periodic forcing, these systems can be referred to as self-sustained systems so that we

can expect to see synchronization-like phenomena in these systems. This phenomenon is known as *stochastic resonance*. Stochastic resonance is a noise-mediated cooperative phenomenon in which noise increases sensitivity to a weak periodic signal when the frequency of the periodic signal matches the intrinsic noise-dependent time-scale of the system (Bulsara et al., 1991; Longtin *et al.*, 1991; Wiesenfeld & Moss, 1995; Gammaitoni *et al.*, 1998). This paradoxical phenomenon has been observed in many systems including bistable ring lasers, semiconductor devices, chemical reactions, and physiological mechanoreceptors in the tail fan of a crayfish (Gammaitoni *et al.*, 1998; Wiesenfeld & Moss, 1995). In order for a system to exhibit stochastic resonance, it needs three minimal ingredients: a) a weak coherent input (e.g. a periodic signal) input, b) a source of stochastic noise that is inherent in the system, or that adds to the coherent, and c) a potential barrier or threshold that needs to be overcome in order to activate the system. These three ingredients must act together in a synergetic manner to exhibit stochastic resonance. When the signal is strong enough to overcome the threshold, optimal amounts of noise added either to the system or the signal may occasionally suffice to trigger activation, therefore the term stochastic resonance (Gammaitoni *et al.*, 1998)

Stochastic resonance can be understood from the synchronization viewpoint. Consider double-well potential well system with two stable equilibria, where the noise induces transitions from one state to the other. This can be represented as a particle in a potential that has two minima (Figure 1). The rate of transition of the particle between the two minima depends on the noise intensity. Small noise induces rare jumps; with increasing noise intensity the transition rate grows. If the noise is too strong, the particle moves back and forth in an erratic manner. A weak external force modifies the double-well potential, making one state more stable than the other. Here weak signal means that it is not strong enough to cause transition, but it increases transition

probability when combined with noise. Transition probability increases when the potential barrier is low. Consequently, for a certain range of noise intensities, noise-induced oscillations appear in approximate synchrony with the periodic force. In this sense, stochastic resonance can be interpreted as synchronization of noise-induced oscillations similar to forced synchronization (Shulgin et al., 1995; Neiman et al., 1998, 1999a, 1999b, 1999c, 2002). The detailed characterization of stochastic resonance will be discussed in chapter 4.

The key observation allowing one to see stochastic resonance as synchronization is the existence of two time scales. One (microscopic) scale is related to the correlation time of the noise; it is small. The other one (macroscopic) is the characteristic time between macroscopic events (jumps in a bistable system); it is much larger than the correlation time of the noise. We are interested in the jumps and the times when they occur. The difference between the two time scales makes it possible for characteristic macroscopic events to occur at any time. By slightly changing the threshold at some instant of time, we can cause a transition at this time. This means that the phase of the macroscopic hopping events can be shifted by weak periodic force, and this is exactly the property yielding synchronization.

#### *The application of synchronization ideas to cognitive processes*

The brain is complex at all levels of organization from the morphology and activity patterns of the individual neurons to the circuitry and population activity of large-scale networks involving millions of neurons. The large-scale activity emerges from the cooperative action of many neurons. As one possible underlying mechanism for large-scale activity, “temporal correlation hypothesis” or “phase synchronization” using the idea of mutual synchronization among neurons was proposed (Gray *et al.*, 1989; Singer & Gray, 1995; Singer, 1999; Varela *et al.*, 2001; Ward, 2003).

Our external sensory environment is also full of ever-changing complex and dynamical signals –glittering neon lights, rippling water, trembling leaves, motion through a textured environment. How does the brain interact with this dynamical sensory environment and give rise to cognitive process? To investigate this problem under the laboratory condition, ever-changing signals can be simplified as periodic luminance modulations. This situation is very similar to the classical example of the entrainment by an external periodic force described in section *forced synchronization* and section *stochastic resonance*. The novel properties of the human brain can be revealed by entraining human visual system with periodically modulated signals as will be shown in Chapter 3 and Chapter 4.

In summary, one may gain insight into how the complex dynamics at different levels of neuronal organization emerges in the human brain by employing the ideas of synchronization theory.

### **3. SYNCHRONIZATION AT ELECTROPHYSIOLOGICAL LEVEL**

#### **Experiment 1 - Attention induces synchronization-based response gain in steady-state visual evoked potentials**

Perceptual abilities vary immensely as a function of where an individual voluntarily allocates attention. How does attention increase sensitivity to visual stimuli that are presented at an attended location? Three competing hypotheses have been proposed to explain how attention modulates the activation of visual cortical networks. According to the contrast gain hypothesis, the effects of attention are equivalent to increasing stimulus contrast. Thus, this hypothesis predicts that attention should cause a leftward shift in the neural contrast-response function. Neural responses grow with increasing stimulus contrast, following a nonlinear sigmoidal contrast-response function. Therefore, attention should boost neural responses when stimulus

contrast is within or below the dynamic range of the neural contrast-response function, but not when stimulus contrast is above the point of response saturation (Figure 1-1A). According to two other hypotheses, the response gain and activity gain models, attention multiplicatively increases the responses of the visual neurons that selectively respond to the attended stimulus. Both of these hypotheses predict that attention should boost neural responses most strongly for stimuli with high contrast (Figure 1-1B). The response and activity gain hypotheses differ in terms of the effects of attention on spontaneous neural activity. The response gain hypothesis postulates that attention multiplicatively increases only the stimulus-driven component of neural responses, predicting that attention should have no effect on spontaneous neural activity, whereas the activity gain hypothesis postulates that attention multiplicatively boosts the net neural activity, including spontaneous activity (Figure 1-1B).

To test these hypotheses, stimulus contrast must be varied from a sub-threshold level to a response-saturation level to obtain full contrast-response functions for attended and ignored stimuli. The contrast gain hypothesis predicts that the effects of attention should be largest for moderate-contrast stimuli (in the middle of the dynamic range), whereas the response and activity gain hypotheses predict that attention effects should be largest for high-contrast stimuli, either with (activity gain) or without (response gain) the boosting of spontaneous activity. Numerous electrophysiological and neuroimaging studies have demonstrated that attention increases neural activity for attended, relative to ignored, stimuli. Fixed stimulus contrasts, however, were typically used in these studies, so that the results are equivocal for evaluating the three hypotheses. Only rarely have the effects of attention on contrast-response functions been examined (Reynolds et al., 2000; Di Russo et al., 2001; Cameron et al., 2002; Ling & Carrasco,

2006; Huang & Dobkins, 2005; Carrasco et al., 2004; Williford & Maunsell, 2006; Morrone et al., 2002; Lee et al., 1999).

For single neurons in areas V4 and MT, several studies reported that voluntary visual attention affected spiking activity, primarily on the basis of contrast gain (Reynolds et al., 2000; Reynolds & Chelazzi, 2004; Martinez-Trujillo & Treue, 2002); attention modulated the later component of responses (B200–450 ms after stimulus onset), even for high contrast stimuli (Reynolds et al., 2000; Fries et al., 2001), but not as strongly as for low- to moderate-contrast stimuli. Recent recordings from a large number of V4 neurons, however, found a variety of attention effects on neuronal contrast response functions. The attention effect on each neuron was partially consistent with contrast, response or activity gain, yielding a statistical tie across the population, but slightly favoring response and activity gain (Williford & Maunsell, 2006). Behavioral results are also mixed with respect to the three hypotheses. Consistent with contrast gain, a recent study (Ling & Carrasco, 2006) reported that voluntary attention improved orientation discrimination for low to moderately high-contrast stimuli, corresponding to the dynamic range of the psychometric function (behavioral performance plotted as a function of contrast). However, attention did not affect performance for high-contrast stimuli, corresponding to the saturated portion of the psychometric function. If attention only operates through mechanisms that induce contrast gain (Figure 1-1A), then attention should be generally ineffective for high-contrast stimuli. Contrary to this prediction, robust behavioral attention effects are generally found with high-contrast stimuli, as such stimuli are more readily detected and processed when presented at the focus of attention (Morrone et al., 2002; Lee et al., 1999; Posner et al., 1980). Furthermore, some behavioral results provide evidence for multiplicative attention effects consistent with response gain (for example, attention improved the

discrimination of contrast, orientation and spatial frequency more for a higher-contrast than for a lower-contrast stimulus) (Morrone et al., 2002; Lee et al., 1999) or evidence for the involvement of both contrast gain and response gain (Huang & Dobkins, 2005). In sum, for both neuronal spike rates and behavioral performance, the evidence to date has been mixed as to whether voluntary visual attention primarily affects neural activity based on contrast (Reynolds et al., 2000; Cameron et al., 2002; Ling & Carrasco, 2006; Huang & Dobkins, 2005; Carrasco et al., 2004; Reynolds & Chelazzi, 2004; Martinez-Trujillo & Treue, 2002), response (Huang & Dobkins, 2005; Williford & Maunsell, 2006; Morrone et al., 2002; Lee et al., 1999), or activity (Williford & Maunsell, 2006) gain.

The three hypotheses have not previously been examined at the level of the neural population. This examination is important for two reasons. First, it is intrinsically difficult to compare the contrast response functions of individual neurons with behavioral results because it is unclear how neural signals from different visual areas (or sub-areas) contribute to performing a specific behavioral task (Maunsell & Cook; 2002). An examination of neural population responses will identify the primary population activity that is induced by a given stimulus and determine how that population activity is affected by allocation of attention to the stimulus. Second, neural population activity takes on emergent characteristics that are not reflected in the spike rates of individual neurons. Response synchronization is one such example, and there is evidence that attention modulates synchronization. For example, visual attention led to increased 35–90-Hz (gamma-frequency) synchronization among V4 neurons that were responding to an attended stimulus (Fries et al., 2001). For another example, attention to tactile (as opposed to visual) stimuli increased the synchronization among somatosensory neurons (Steinmetz et al., 2000). Because the synchronization can increase the impact of the involved neurons on

postsynaptic targets (Azouz & Gray, 2000), these results suggest that response synchronization is one of the mechanisms that are important for attentional selection (Niebur & Koch, 1994; Buia & Tiesinga, 2006). Recent evidence suggesting that the coding of stimulus contrast in V1 involves synchronization (Henrie & Shapley, 2005) is also consistent with a function for neural response synchronization in modulating the strength of stimulus representation. Because response synchronization is not limited by the saturation of neuronal spike rates at high contrasts (Henrie & Shapley, 2005), we hypothesized that attentional modulations of the coherence of neural population responses might provide a mechanism that is especially effective for increasing the salience of high-contrast stimuli. This would complement the attentional modulations of neuronal spike rates, which may be potentially limited by response saturation at high contrast.

Our strategy for investigating the effects of attention on the coherence of neural population activity in humans was to monitor SSVEPs that were elicited by flickering stimuli (Regan, 1989). These electroencephalographic (EEG) measures can index the increased synchronization of neural responses even if the firing rate of individual neurons is saturated because of high contrast. Hypothetically, if attention induced contrast gain in individual neurons, while also inducing multiplicative response (or activity) gain in terms of increased phase locking of population activity to stimulus flicker, SSVEP amplitudes might be sensitive enough to demonstrate response (or activity) gain. Indeed, some of the data reported in a prior SSVEP study (Di Russo et al., 2001) are suggestive of multiplicative attention effects on SSVEP amplitudes. Here we rigorously tested the attentional response and activity gain hypotheses for neural population activity by recording frequency-tagged SSVEPs from both attended and ignored stimuli simultaneously (thus controlling for influences on SSVEPs that were unrelated to attention), analyzing the scalp topography of attention effects (crucial for evaluating the

attentional response and activity gain hypotheses) and examining the effects of attention on response synchronization.

The response and activity gain hypotheses predict that attention directly boosts visual responses that are elicited by the attended stimulus (Figure 1-1B). Evidence in support of these hypotheses must demonstrate that there is a multiplicative attention effect on population activity that is stimulus selective. Therefore, we recorded frequency-tagged SSVEPs from numerous scalp locations to identify patterns of activity that were specific to each of the competing stimuli. We then sought to demonstrate that attentional boosts in SSVEP amplitudes occur with a topographic pattern that is indicative of the selective enhancement of sensory activation and that this enhancement is multiplicative (Figure 1-1B). The presence or absence of attention effects on subthreshold activity allowed us to distinguish between response and activity gain.

Care must be taken to ensure that SSVEP modulations can clearly be attributed to selective attention. This requires that attended and ignored conditions be equated in terms of arousal and the type of visual processes engaged. Accordingly, we presented two flickering circular gratings, one to be attended to and the other to be ignored, in the left and right visual hemifields (Figure 1-2A). When the observer attended to one grating, he or she simultaneously ignored the other grating, such that the level of arousal and general task requirements were comparable while we recorded SSVEPs from both the attended and ignored gratings simultaneously (Morgan et al., 1996). We made two gratings flicker at different frequencies so that the Fourier band-power value for each frequency could be extracted from the EEG activity to measure coherent neural responses to the respective gratings separately (Morgan et al., 1996; Müller et al., 2003; Müller et al., 2003). This frequency-tagging method allowed us to simultaneously monitor SSVEPs from attended and ignored stimuli so that we could determine

whether attentional modulation of stimulus selective population electrophysiological activity (recorded as EEG) reflected contrast gain (Figure 1-1A), response gain or activity gain (Figure 1-1B).

We found that (i) each grating elicited SSVEPs that were localized in the contralateral posterior scalp region, (ii) voluntary visual attention selectively and multiplicatively boosted these stimulus-induced SSVEPs in a manner that was consistent with response gain and (iii) this attentional boosting was at least partially attributable to the enhancement of neural response synchronization by attention.

*Observers:*

Eight observers with normal or corrected-to-normal vision participated as paid volunteers after giving informed written consent. The group included five men and three women. Their ages ranged from 23 to 45 years.

*Stimuli:*

We displayed stimuli on a 19-inch CRT monitor set to a 100-Hz refresh rate. We presented two identical square-wave modulated circular gratings (1.1 cycles per degree in fundamental spatial frequency) to the left and right visual hemifields (Figure 1-2A). We always flickered the two gratings at different frequencies (12.50 Hz and 16.67 Hz, with assignment to visual hemifield randomized across trials). We induced flicker by modulating the luminance of the concentric rings symmetrically (darker and lighter) against the mid-gray ( $64.7 \text{ cd m}^{-2}$ ) background, which prevented the creation of negative afterimages. Because visual neurons are primarily driven by luminance changes, we define the contrast,  $C$ , of the flickered gratings as,  $C = (L_{light} - L_{dark}) \times (L_{light} + L_{dark})^{-1}$ , where  $L_{light}$  and  $L_{dark}$  indicate the luminance during the light and dark phases, respectively.

*Experimental procedure:*

The observer initiated each trial by a button press (Figure 1-2B). A central arrow (attention cue) then appeared for 2 s to indicate which grating (left or right) the observer was to attend to during that trial. Following a 1-s fixation screen, the two flickering gratings appeared. During the subsequent 4.8-s period, the observer voluntarily attended to the cued grating, while maintaining eye fixation at the central fixation marker and attempting to withhold blinks. We directly manipulated attention by instructing the observers to sustain attention to the cued grating and ignore the other grating. We chose this method, rather than indirectly manipulating attention by using a visual task, so that SSVEP modulations could be attributable to voluntary spatial attention without potential task-related confounding factors. Behavioral (Ling & Carrasco, 2006; Posner et al., 1980; Sperling & Melchner, 1978; Suzuki, 2001) as well as fMRI (O'Craven et al., 1997) results have provided evidence that human observers can reliably allocate attention when instructed to do so. The fact that we obtained substantial attentional boosting of stimulus-selective contralateral SSVEPs provides evidence that our observers successfully allocated attention to the cued grating.

To verify that our manipulation of attention produced behavioral effects that were independent of grating contrast, we conducted the following control experiment. The trials were identical to those in the SSVEP experiment (Figure 1-2B), except that we presented a cue instructing the observer to attend to both gratings on half of the trials and we measured the effects of attention using a probe display that was flashed for 100 ms. We presented the probe display (Figure 1-8) 500 ms after the grating onset, as the time course of ITPC (Figure 1-6B) indicated that observers fully allocated their attention by 500 ms. The target in the probe display was defined by a pair of oblique lines, identical in orientation, that occurred at the location of

one of the gratings. The target always occurred at the location of the attended grating when the observer attended to only one grating (cue validity was 100%). Because we presented the targets among feature-matched distractors, they did not attract attention, nor were they easily detectable when the observer distributed attention across the display (Treisman & Sato, 1990). Thus, the experiment provided a sensitive measure of attention allocation, where successfully focused attention should have resulted in faster and more accurate target detection at the location of the cued grating. We adjusted the contrast of the probe display for each grating contrast and for each observer so that the target-detection performance in the distributed-attention condition was equivalent for all of the grating contrasts. We tested three of the eight observers who participated in the SSVEP experiment, using 5%, 20% and 80% randomly intermixed grating contrasts, with 384 trials per observer. All of the observers produced both faster response time and greater accuracy in the focused-attention condition (while attending to only one grating) than in the distributed-attention condition (while attending to both gratings) for all of the grating contrasts. Average response times were: 769 ms (focused) versus 982 ms (distributed) for the 5% contrast grating (a 213-ms advantage), 831 ms versus 950 ms for the 20% contrast grating (a 119-ms advantage) and 781 ms versus 972 ms for the 80% contrast grating (a 191-ms advantage). Average accuracies were: 85% (focused) versus 73% (distributed) for the 5% contrast grating (a 12% advantage), 85% versus 74% for the 20% contrast grating (an 11% advantage) and 89% versus 73% for the 80% contrast grating (a 16% advantage). Thus, these results verified that our instructional manipulation of attention produced similar behavioral effects at different grating contrast levels, suggesting that our observers allocated a comparable amount of attention to gratings of different contrasts. In the SSVEP experiment, there were 32 trial types: 2 directions of attention (left or right), 2 assignments of flicker frequencies (12.50 Hz on the left and 16.67

Hz on the right, and vice versa) and 8 contrast levels (0.00625, 0.0125, 0.025, 0.05, 0.10, 0.20, 0.40, or 0.80). We ran each trial type 20 times while randomly varying and counterbalancing the 3 factors across trials. We tested each observer for a total of 640 trials in blocks of 160 trials. We initially ran several practice trials and also gave breaks as necessary.

*Data recording and analysis:*

We recorded EEG activity using tin electrodes embedded in an elastic cap at locations distributed relatively evenly across the scalp. For 59 EEG channels, the right mastoid served as the reference. We used four additional channels for monitoring vertical and horizontal electro-oculographic (EOG) activity. We lowered electrode impedances to 5 k $\Omega$ , amplified signals with a bandpass of 0.3–200 Hz and digitized them at 1,000 Hz.

We rejected individual trials from further analysis on the basis of blink or muscle-activity artifacts detected by vertical EOG activity. In addition, to retain only the trials in which central eye fixation was maintained, we recursively rejected trials with the highest horizontal EOG activity until the average horizontal EOG activity for each condition (defined by each combination of attention allocation, flicker-frequency assignment, and contrast) for each observer was less than 5  $\mu$ V during the entire 4.8-s trial period. This criterion approximately corresponds to maintained central fixation within a visual angle (Müller et al., 1998a; Luck et al., 1994) of 0.5°. Following these artifact-rejection procedures, we retained a mean of 89% of the trials.

To exclude the initial transient response to the grating onset, we analyzed EEG waveforms recorded from 526 ms to 4,621 ms after grating onset (except for the time course analysis of ITPC which included the entire trial period). This yielded 4,096 ( $2^{12}$ ) data points per trial. Reducing the number of EEG data points from each trial to a power of 2 is optimal for fast

Fourier transform (FFT) analysis. We averaged EEG waveforms from the 59 scalp electrodes separately for each condition and for each observer and then we re-referenced the average waveforms to the average of left and right mastoid recordings.

To extract SSVEP activity that was synchronized to the stimulus flicker, we subjected each re-referenced average waveform (corresponding to a specific condition) from each scalp electrode to an FFT. We then computed the SSVEP amplitude as the Fourier band-power within the range of 0.976 Hz centered at the second harmonic of the stimulus flicker frequency. Because the luminance flicker we used was symmetric about the mid-gray background (Figure 1-2), the fundamental-frequency responses (for example, first harmonic) from the non-frequency doubling cortical simple cells would have mostly averaged out in SSVEPs due to the random spatial distribution of the ON and OFF sub-regions of their receptive fields with respect to the flickered stimuli (Di Russo et al., 2001; Campbell & Maffei, 1970; Hou et al., 2003; De Valois et al., 1982). Any remaining power at the fundamental frequencies would then be due to overall unequal activation of the ON and OFF sub-regions, unbalanced amplitudes of ON and OFF responses or both. The effects of attention on such residual responses would be difficult to interpret. In contrast, frequency-doubling responses from cortical complex cells<sup>50</sup> are largely spatial-phase invariant and they contribute robustly to SSVEPs (Campbell & Maffei, 1970; Hou et al., 2003).

Because the absolute values of EEG signals vary widely from observer to observer, we standardized the data from the eight observers before combining them. Specifically, we z-transformed the SSVEP amplitude from each electrode, in each condition and for each observer based on the observer's overall average and standard deviation of SSVEP amplitudes across all scalp electrodes and across all of the conditions.

*Results:*

We elicited SSVEPs by using circular gratings flickering at 12.5 Hz and 16.67 Hz. Two gratings appeared simultaneously in the left and right visual hemifields (Figure 1-2A), with flicker frequency randomly assigned to each hemifield on each trial. Each trial lasted 4.8 s, during which the observer maintained fixation at a central marker while voluntarily attending to the grating that was indicated by a central arrow that was presented prior to each trial (Figure 1-2B). We contrasted SSVEPs that were derived from the second-harmonic EEG responses (see Date recording and analysis) for attended and ignored conditions.

The SSVEP topographies for the responses to the 16.67-Hz grating (Figure 1-3A) showed that the maximal SSVEP amplitudes occurred contralateral to the stimulus over posterior cortical regions and that attention boosted these localized responses. The topography of the SSVEP differences between the attended and ignored conditions showed that the contralateral posterior focus of attentional enhancement closely resembled the SSVEP topographies for the attended and ignored conditions. This topographic similarity between SSVEP responses and SSVEP enhancement suggests that the attentional modulation occurred in the same brain regions that were selectively activated by the grating. A parallel set of results for SSVEPs that were synchronized to the 12.50-Hz grating (Figure 1-3B) showed a similar pattern, except that the SSVEP amplitudes were generally larger.

These findings demonstrated that the stimuli elicited focal SSVEPs at contralateral posterior scalp regions and that voluntary spatial attention boosted these localized visual responses. We next evaluated whether this attentional boost of stimulus-evoked population electrophysiological activity was consistent with contrast gain (Figure 1-1A), response gain or activity gain (Figure 1-1B). To evaluate SSVEP contrast-response functions, we used data from

ten scalp locations (five on each side of the scalp; Figure 1-4A) that were selected to correspond to the foci of maximal sensory activation and attentional boost. We averaged SSVEPs separately for locations contralateral and ipsilateral to the side of stimulation (combining left and right stimulus presentations).

For SSVEPs that were elicited by the 16.67-Hz grating, the contralateral contrast-response functions for the attended and ignored conditions showed that the effect of attention monotonically increased with increasing stimulus contrast, with attention having no effect at the lowest contrasts (Figure 1-4B). This finding is consistent with the response gain hypothesis (Figure 1-1B). To quantitatively confirm the multiplicative attention effect, we first fit both the attended and ignored contrast-response functions using the Naka-Rushton equation, which is typically used to fit neural contrast response functions (Figure 1-4). If attention multiplicatively boosted visual responses, then the difference between the attended and ignored contrast-response functions should also be well fit by the Naka-Rushton equation<sup>1</sup>. This was indeed the case (Figure 1-4B;  $F_{1,7} = 41.582$ ,  $P < 0.001$ ). Attention had negligible effects on the weak responses recorded from ipsilateral locations, which confirmed the spatial selectivity of the attention effect (Figure 1-4B).

We found essentially the same pattern of results for SSVEPs that were elicited by the 12.50-Hz grating (Figure 1-4C). The attentional boosting of SSVEPs was spatially selective (confined to contralateral locations) and the contrast-response functions indicated response gain; the difference between the attended and ignored contrast-response functions grew monotonically with increasing stimulus contrast, conforming to the Naka-Rushton equation (Figure 1-4C;  $F_{1,7} = 9.107$ ,  $P < 0.02$ ), with attention having no effect at the lowest contrasts.

In addition to these primary results that consistently supported the idea that the effects of attention on SSVEPs have response gain characteristics, we also found some frequency dependencies. First, SSVEPs were generally stronger for the 12.50-Hz grating than for the 16.67-Hz grating (compare Figures 1-3A and 1-3B). This could be related to differences in perceived contrast. Although the amplitude of luminance modulation was physically identical for the two flicker frequencies, subjectively the 12.50-Hz grating appeared slightly higher in contrast than the 16.67-Hz grating, probably owing to a higher perceptual sensitivity to the slower flicker. Second, the effects of attention were generally greater for the 16.67-Hz grating than for the 12.50-Hz grating (compare Figures 1-4B and 1-4C). Indeed, the magnitude of the attention effects might depend systematically on flicker frequency<sup>24</sup>. We note that the examined EEG second-harmonic responses (33.33 Hz) were in the gamma range for the 16.67-Hz grating and that some evidence suggests that gamma-range synchronization is closely associated with attention (Fries et al., 2001; Fell et al., 2003). Third, within the contrast range used, SSVEP contrast response functions saturated for the 16.67-Hz grating (Figure 1-4B), but not for the 12.50-Hz grating (Figure 1-4C). Perhaps the higher-frequency grating activated a higher ratio of magno-type to parvo-type neurons than did the lower-frequency grating. Magno-type neurons may disproportionately contribute to the perception of a faster flicker (Schiller et al., 1990; but see Levitt et al., 1994; Hawken et al., 1996) and they also tend to saturate at a lower contrast (Edwards et al., 1995).

These frequency dependencies merit further investigation, and it is unclear how SSVEP results might differ for frequencies that were not tested in this experiment. Nevertheless, our SSVEP results provided strong evidence that is pertinent to the response gain hypothesis. Both the 16.67- and 12.50-Hz gratings elicited electrophysiological responses that were localized to

the contralateral posterior scalp regions, and attention boosted these focal responses in a manner that was consistent with the response gain hypothesis.

*Discussion:*

To understand how the voluntary allocation of spatially focused attention modulates neural activity, previous research has considered three hypotheses: contrast gain (the effects of attention being equivalent to increasing stimulus contrast), response gain (attention multiplicatively boosting stimulus-evoked neural activity) and activity gain (attention multiplicatively boosting the net neural activity). As discussed above, to date the evidence at the level of single neurons has been mixed. Here we investigated these hypotheses at the neural population level by using flickered stimuli and monitoring the corresponding SSVEPs. Voluntary visual attention multiplicatively increased the synchronized electrophysiological activity, which likely arose from contralateral neocortical regions in response to these stimuli. As attention did not affect the baseline activity, we have demonstrated attentional response gain at the neural population level.

There are at least two possible ways by which attention could increase SSVEPs in accord with response gain, even if attention increased neuronal spike rates predominantly in accord with contrast gain. First, a response gain pattern might emerge for a neural population when responses are averaged across neurons with a variety of contrast response functions (showing different half-saturation contrasts and maximum responses) and various magnitudes of attention-based contrast gain. Note that we cannot make any firm predictions about SSVEPs on the basis of single-cell spike rate activity because SSVEPs reflect aggregate local field potentials, which are more closely associated with the synaptic activity of a neural population than with spike rates (Henrie & Shapley, 2005; Varela et al., 2001). Nevertheless, we conducted a simulation analysis

to show that attentional response gain at the population level cannot emerge from a linear summation of attentional contrast gain on single-cell spike rate activity. We assumed that each neural contrast-response function was reasonably approximated by the Naka-Rushton equation (a neural response,  $R$ , as a function of contrast,  $C$ ; equation (1)) (Geisler & Albrecht, 1997) and that the parameters  $a$  (maximum response relative to baseline),  $C_{50}$  (half-saturation contrast),  $n$  (steepness of the contrast response function) and  $b$  (spontaneous baseline response) were normally distributed across the responding population of neurons.

$$R(C) = a \frac{C^n}{C^n + C_{50}^n} + b \quad (1-1)$$

We considered a wide range of population means and standard deviations for the distributions of these contrast-response parameters, including published values for monkey V1 (Geisler & Albrecht, 1997) and V4 (Williford & Maunsell, 2006) neurons. In simulating the effects of attention, we assumed that the magnitude of attentional contrast gain (the reduction in the  $C_{50}$  parameter with attention) was normally distributed across the responding neurons, and we tested a wide range of population means and standard deviations for the attention effect (the mean percentage reduction in  $C_{50}$  was varied from 0% (no attentional contrast gain) to 100% (maximum attentional contrast gain) with the standard deviations ranging from 0% to 1,000%). For each simulated neural population, we computed the average attention effect (the difference between attended and ignored responses) as a function of contrast. All of our simulated population-averaged attention effects peaked at mid-range contrasts (Figure 1-5), consistent with contrast gain (Figure 1-1A). This indicates that the average population responses from neurons with a variety of contrast-response functions and attentional contrast gain magnitudes should still produce an overall contrast gain effect. Thus, it is unlikely that the attentional response gain

effects we observed on SSVEPs were due to the simple averaging of contrast gain effects from individual neurons.

An alternative possibility is that attention increases the phase coherence of neural responses at the population level, in addition to producing contrast gain or a mixture of contrast, response and activity gain at the neuronal level. Because SSVEPs are measured as frequency-locked electrophysiological responses to flickered stimuli, increased SSVEPs could arise from increased amplitudes or from an increase in the coherence of underlying neural responses (Rager & Singer, 1998; Srinivasan et al., 1999). One way to evaluate whether attention increased neural response synchronization is to examine intertrial phase coherence (ITPC) (Tallon-Baudry et al., 1996; Delorme & Makeig, 2004). ITPC provides an amplitude-independent measure of the degree to which stimulus-evoked EEG responses are phase-locked to the stimulus volleys. For example, when the neuronal responses underlying SSVEPs are not synchronized, there will be substantial random variability in the phase lags among those responses, producing SSVEPs with large variability in phase from one stimulus volley to another. In contrast, when the neuronal responses underlying SSVEPs become more synchronized to stimulus dynamics, there will be less random variability in the phase lags among those responses, producing coherent SSVEPs with less variability in phase from one stimulus volley to another. ITPC provides a measure of this phase consistency in terms of the degree to which EEG responses of a specific frequency are time-locked to stimulus dynamics. ITPC values vary from 0 (a complete absence of synchronization) to 1 (perfect synchronization).

Voluntary attention increased the average ITPC in the contralateral focal electrodes by 10% for both 16.67-Hz and 12.50-Hz gratings at the higher end of the stimulus contrast range (40% and 80%; Figure 1-6A). The time course of the ITPC (averaged across 40% and 80%

contrasts) shows that the effect of attention emerged within 300–500ms (Figure 1-6B), which is within the temporal range of voluntary attention effects reported for single-cell spike rates (Reynolds et al., 2000; Fries et al., 2001; Reynolds et al., 1999; Chelazzi et al., 1998).

A previous single-cell study (Fries et al., 2001) reported faster (within 50–150 ms) attentional boosting of gamma-range synchronization (and reduction of low-frequency synchronization) between single-cell spikes and local field potentials in V4. It is possible that it takes longer for synchronization to develop over the large population of neurons that generate SSVEPs. Additionally, the two studies examined different types of neural synchronization; whereas the single-cell study found attentional modulations of local neuronal synchronizations within intrinsic frequencies, we found attentional enhancement of population synchronization to stimulus dynamics. Future research is necessary to clarify the relationship between these two types of synchronization. We also acknowledge the need to be cautious in comparing SSVEP results with single-cell results. Specifically, single-cell studies have examined attention effects when stimuli are presented within the neurons' classical receptive fields, whereas SSVEPs combine responses from a large population of neurons, including those for which the stimulus falls on the border of, or outside, their classical receptive fields. Future single-cell research, in which attention effects are examined using large stimuli spanning multiple receptive fields, would be necessary to understand how our SSVEP results relate to attention effects on single neurons.

An important aspect of our results is that the attentional boosting of ITPC increased with contrast, indicating that attention enhanced population synchronization most strongly for high-contrast stimuli (Figure 1-7). This response gain–type attentional enhancement of ITPC occurred throughout the time period of sustained attention (200–400-ms, 400–1,000-ms and 1,000–4,800-

ms intervals), except for the initial period (50–200 ms), in which no attentional modulation of ITPC occurred (Figure 1-7). Overall, converging evidence from our simulation (Figure 1-5) and ITPC analyses suggests that the observed attention-based multiplicative boost in SSVEPs is attributable to attentional modulation of neural response synchronization. Further research will be necessary to understand how voluntary attention increases neural response synchronization, but a recent computational study suggests that one possible mechanism might be for attention to reduce the driving current to inhibitory neurons (Buia & Tiesinga, 2006).

Our results might be criticized on the grounds that natural images are not flickered. In fact, rapid luminance modulations frequently occur in both natural and artificial environments—rippling water, motion through a textured environment, rapid saccades, micro saccades that always occur even during voluntary eye fixation<sup>38</sup>, TV displays and artificial illuminations that generate periodic flicker. Thus, one might argue that flickered stimuli are more ecologically valid (Müller et al., 2003) than the briefly flashed stimuli that are often used in visual attention research. Furthermore, our ITPC analysis has shown that attention increases phase-locking of SSVEPs to rapid changes in luminance, suggesting that attention increases the synchronization of neural population responses to dynamic signals from an attended stimulus. Because retinal stimulation is nearly always dynamic, it is plausible that the synchronization-based multiplicative attention mechanism demonstrated here is also operational in natural situations.

To conclude, visual sensitivity is enhanced for stimuli presented at the focus of attention. Many previous studies have investigated the neural mechanisms underlying the beneficial effects of attention on performance. The present findings add to this body of research by implicating separate functions for the effects of attention on neural population activity and neuronal spike rate activity.

On a fine spatial scale—that is, when attended and ignored stimuli activate many of the same neurons—attention appears to increase the influence of the attended stimulus relative to the influence of the ignored stimulus in determining neuronal activity. This mechanism has been formalized in the biased-competition model (Reynolds et al., 1999; Kastner & Ungerleider, 2001). In this model, attention can affect the relative weighting of signals from attended and ignored stimuli and can mediate attention effects on high-contrast and low-contrast stimuli if both attended and ignored stimuli fall within a single receptive field. For example, when a high-contrast preferred stimulus and a high-contrast null stimulus both fall within a single neural receptive field, attention can boost the neuron’s response by preferentially weighting the signal from the preferred stimulus and can reduce the neuron’s response by preferentially weighting the signal from the null stimulus; the response would be intermediate if both stimuli were ignored. Some suggest that this biased-competition mechanism is closely associated with contrast gain because both selective attention and the relative contrast of competing stimuli similarly modulate the relative influence from within-receptive-field stimuli (Reynolds et al., 2004; Martinez-Trujillo & Treue, 2002). A biased competition–contrast gain mechanism can thus mediate attentional boosts in visual sensitivity for low- to moderate-contrast stimuli in general (Figure 1-1A) and also for high-contrast stimuli when the competing stimuli are near enough to activate a single receptive field. Note that increasing neuronal activity via response or activity gain would be ineffective for selecting among within-receptive-field stimuli; in that case, input modulation would be necessary to accomplish attentional selection, either via contrast gain or via response (or activity) gain occurring in the previous processing stage in which the competing stimuli fall in separate receptive fields.

The biased competition–contrast gain mechanism, however, would be ineffective when attended and ignored stimuli were both high contrast and presented relatively far apart, so as not to fall within a single neuron’s receptive field. For example, in our experiment, the two gratings were presented in opposite visual hemifields. The attended and ignored gratings would have activated separate receptive fields in nearly all of the cortical visual areas throughout the ventral pathway (V1, V2, V4, through the inferotemporal cortex) thought to be closely associated with object perception and pattern visibility (Mishkin et al., 1983; Leopold & Logothetis, 1999; Grill-Spector & Malach, 2004). Even in the inferotemporal cortex, where visual neurons have very large receptive fields, neurons respond primarily to contralateral stimuli regardless of the direction of attention (Chelazzi et al., 1998). In such circumstances, our results implicate a synchronization-based attention mechanism that multiplicatively enhances population neural activity.

In summary, a biased competition–contrast gain mechanism can modulate neuronal spike rates for both low- to moderate-contrast stimuli and spatially proximate stimuli (regardless of contrast). Subpopulations of neurons showing response and activity gain properties may extend attention effects across a broader range of contrasts (Williford & Maunsell, 2006). However, an additional synchronization-based response gain mechanism, operating at the neural population level, allows robust attentional selection of the high-contrast stimuli typically encountered in everyday life even when attended and ignored stimuli are too far apart to be detected by the same neuron’s receptive field. Both neuronal and synchronization-based mechanisms of attention may operate concurrently to fulfill the demands of attentional regulation in diverse environmental circumstances.

**Experiment 2 – Parallel visual processing revealed by evoked oscillatory neural harmonics**

Parallel processing streams are a fundamental characteristic of the visual system. They allow separate, often conflicting, computations to be concurrently performed on sensory signals. Classic examples include magno (extracting temporal information) versus parvo (extracting spectral information) pathways (e.g., Merigan & Maunsell, 1993; Schiller et al., 1990; Shapley, 1995; Yoshikawa et al., 1994), and dorsal (extracting spatial, spatio-temporal, and action-related information) versus ventral (extracting object information) streams (e.g., Goodale et al., 1991; Goodale & Westwood, 2004; Fang & He, 2005; Mishkin, Ungerleider, & Macko, 1983; Ungerleider & Mishkin, 1982).

Here we report potential parallel processing based on neural response harmonics. Because the visual environment is dynamic, responses of visual neurons typically include a broad range of temporal frequencies. To understand how visual neurons respond to dynamic stimuli, periodic stimuli (e.g., flickered patterns, drifting gratings) have typically been used to systematically characterize how visual neurons respond to individual Fourier components. Harmonic responses are observed as early as in V1 where the simple cells typically respond at the flicker frequency (1<sup>st</sup> harmonic) whereas the complex cells typically respond at twice the flicker frequency (2<sup>nd</sup> harmonic) (e.g., De Valois et al., 1982; Hubel & Wiesel, 1968; Levitt et al., 1994). These harmonic responses (neural responses at integer multiples of the flicker frequency) have been observed in many areas of the brain (e.g., Rager & Singer, 1998), and are also prevalent in neural population responses measured with scalp electrodes, known as steady-state visual-evoked potentials (SSVEPs) (e.g., Di Russo et al., 2007; Hermann, 2001; Kim et al., 2007).

Given the ubiquity of harmonic responses, it is reasonable to speculate that different harmonics may support separate processes in response to conflicting behavioral demands. We

investigated this possibility by analyzing SSVEPs elicited by a broad range of flicker frequencies in human observers using 64 scalp electrodes. We analyzed the first two harmonics because SSVEP amplitudes, and corresponding signal-to-noise ratios, diminish for higher harmonics (e.g., Hermann, 2001).

We sought evidence of functionally distinct parallel processes mediated by the 1<sup>st</sup> and 2<sup>nd</sup> harmonics by focusing on SSVEP topography and top-down modulations. We first determined whether the 1<sup>st</sup> and 2<sup>nd</sup> harmonics exhibited anatomically segregated foci of activation as anatomical segregation generally implies functional segregation. We then determined whether the two harmonics resolved conflicting functional demands. We focused on attention effects because not only does attention play a fundamental role in signal selection (e.g., Desimone & Duncan, 1995; Kastner & Ungerleider, 2000), but attentional modulation of neural activation also imposes conflicting demands on visual processing. Whereas strong top-down modulation of neural responses is desirable for the purpose of stimulus selection, such modulation must occur without substantially distorting information about the intensity (e.g., contrast) of visual stimuli. We examined the possibility that the 1<sup>st</sup> and 2<sup>nd</sup> harmonics might segregate these conflicting demands. In other words, one harmonic might be especially susceptible to top-down attentional modulations —mediating attention effects— whereas the other harmonic might be relatively immune to attentional modulations —preserving undistorted sensory qualities.

Our experiments yielded three key findings. First, the 1<sup>st</sup> and 2<sup>nd</sup> harmonics were topographically segregated in EEG recordings, with the 1<sup>st</sup> harmonic most prominent in the medial posterior scalp regions whereas the simultaneously generated 2<sup>nd</sup> harmonic most prominent in the contralateral posterior scalp regions. Second, this topographic segregation was harmonic specific and frequency independent within a broad range of flicker frequencies (~8.33

Hz to 25 Hz). Third, voluntary spatial attention strongly modulated the 2<sup>nd</sup> harmonic without significantly modulating the 1<sup>st</sup> harmonic.

We focused on the first two harmonics because SSVEP amplitudes, and corresponding signal-to-noise ratios, diminish for higher response frequencies (Regan, 1989). To investigate the possible topographic segregation of the two harmonics, we analyzed SSVEP topographies resulting from a broad range of stimulus flicker frequencies. To investigate the potential functional differences between the two harmonics, we analyzed attentional modulations of those harmonics.

The topographic analysis focused on the extent to which the contralateral organization of visual processing was reflected in the 1<sup>st</sup> and 2<sup>nd</sup> harmonics of SSVEPs. To examine SSVEP topography independent of the specific flicker frequency, we compared the 1<sup>st</sup> and 2<sup>nd</sup> harmonics elicited by multiple flicker frequencies. For example, a 25-Hz SSVEP can be produced as the 1<sup>st</sup> harmonic by a 25-Hz flicker or as the 2<sup>nd</sup> harmonic by a 12.5-Hz flicker.

Further analysis focused on the possibility that attention might preferentially modulate one of the two harmonics. We speculated that one harmonic might be strongly modulated by attention, mediating top-down modulations of sensory signals, whereas another harmonic might be relatively unaffected by attention, preserving sensory information. In this way, strong top-down modulations of sensory signals can be accomplished while simultaneously preserving undistorted sensory information.

Our experiments yielded three key findings. First, the 1<sup>st</sup> harmonic was most prominent in EEG recordings from medial posterior scalp regions whereas the simultaneously generated 2<sup>nd</sup> harmonic was most prominent in EEG recordings from contralateral posterior scalp regions. Second, this topographic segregation was harmonic specific and frequency independent within a

broad range of flicker frequencies (~8.33 Hz to 25 Hz). Third, voluntary spatial attention strongly modulated the 2<sup>nd</sup> harmonic without significantly modulating the 1<sup>st</sup> harmonic.

*Observers:*

Twelve observers (9 men and 3 women, ages ranging from 23 to 46) participated in the primary experiment; data from two observers (1 man and 1 woman) were excluded from the analyses due to excessive blinking. Eight observers (5 men and 3 women, ages ranging from 23 to 45) participated in the attention experiment (the 2<sup>nd</sup> harmonic data reported in Kim et al., 2007). All observers had normal or corrected-to-normal visual acuity, gave informed consent to participate as paid volunteers, and were tested individually in a dimly lit room.

*Stimuli:*

Square-wave modulated circular gratings (1.1 cycle/degree in fundamental spatial frequency) were shown on a 19" CRT monitor set to a 100-Hz refresh rate (Figure 2-1). The diameter and retinal eccentricity of each grating was 5.9° and 4.47°, respectively.

Each grating was presented against a mid-gray background (64.7 cd/m<sup>2</sup>) and was flickered at different frequencies, 6.25 Hz, 8.33 Hz, 12.5 Hz, 16.67 Hz, or 25 Hz in the main experiment, and 12.5 Hz or 16.67 Hz in the attention experiment. Flicker was generated by modulating the luminance of the concentric rings symmetrically (darker and lighter) against the mid-gray background, which prevented the creation of negative afterimages, produced no sensation of motion (unlike counterphase flickered gratings), and produced robust SSVEPs at both the 1<sup>st</sup> and 2<sup>nd</sup> harmonics. Because visual neurons are primarily driven by luminance changes, we define the contrast,  $C$ , of the flickered gratings as,  $C = \frac{L_{light} - L_{dark}}{L_{light} + L_{dark}}$ , where  $L_{light}$  and

$L_{dark}$  indicate the luminance during the light and dark phases, respectively. The contrast was 0.80

in the main experiment. The contrast was varied between 0.0625 and 0.80 in the attention experiment (see Kim et al., 2007).

*Experimental Procedure:*

Each trial was initiated by the observer's button press. In the main experiment, a single grating was presented on each trial either in the left or right visual hemifield. The hemifield and flicker frequency of the grating (6.25 Hz, 8.33 Hz, 12.5 Hz, 16.67 Hz, or 25 Hz) were randomly intermixed across the 300 trials, and each condition occurred with an equal probability. Several practice trials were given initially and breaks were provided as appropriate. The grating was presented following 1 sec of a fixation screen displaying a central bull's eye. The flickered grating lasted 4.8 sec during which time the observer attempted to maintain eye fixation at the central fixation marker and withhold eye blinks.

In the attention experiment, two gratings were presented, one in the left and the other in the right visual hemifield. One grating flickered at 12.5 Hz and the other at 16.67 Hz. Assignment of frequency to visual hemifield was randomized across trials. An arrow cue presented in the initial fixation screen indicated to the observer the grating to which he or she voluntarily attended during the 4.8-sec period (see Kim et al., 2007 for additional details).

*Data Recording and Analysis:*

Electroencephalographic activity was recorded using tin electrodes embedded in an elastic cap at locations distributed relatively evenly across the scalp. For 59 EEG channels, the right mastoid served as the reference. Four additional channels were used for monitoring vertical and horizontal eye movements in order to reject trials contaminated by electro-oculographic (EOG) artifacts. Electrode impedances were lowered to 5 k $\Omega$ . Signals were amplified with a bandpass of 0.3 –200 Hz and digitized at 1000 Hz.

Individual trials were rejected from further analysis on the basis of blink or muscle-activity artifacts detected by vertical EOG activity. In addition, to retain only the trials in which central eye fixation was maintained, we recursively rejected trials with the highest horizontal EOG activity until the average horizontal EOG activity for each condition (i.e., each flicker frequency presented to each visual hemifield) for each observer was less than 5  $\mu\text{V}$  during the entire 4.8-sec trial period. This criterion approximately corresponds to central fixation within  $0.5^\circ$  visual angle (Müller et al., 1998a; Luck et al., 1994). Following these artifact-rejection procedures, we retained a mean of 88% for the main experiment and 89% for the attention experiment.

To exclude the initial transient response to the grating onset, we analyzed EEG waveforms recorded from 526 ms to 4621 ms after grating onset. This yielded 4096 ( $2^{12}$ ) data points per trial. Reducing the number of EEG data points from each trial to a power of 2 is optimal for Fast Fourier Transform (FFT) analysis. EEG waveforms from the 59 scalp electrodes were averaged separately for each condition for each observer, and were then re-referenced to the average of left and right mastoid recordings.

To extract SSVEP activity synchronized to the stimulus flicker, each re-referenced average waveform (corresponding to a specific condition) from each scalp electrode was subjected to an FFT. The SSVEP amplitude was then computed as the Fourier band-power within the range of 0.976 Hz centered at the 1<sup>st</sup> and the 2<sup>nd</sup> harmonic of the stimulus flicker.

Because the absolute values of EEG signals vary widely from observer to observer, partly due to individual differences in scalp conductivity, data were standardized prior to combining across observers. The SSVEP amplitude from each electrode in each condition for each observer was  $z$ -transformed based on the observer's overall average and standard deviation of SSVEP

amplitudes across all scalp electrodes and all conditions. We normalized each harmonic separately so that we could evaluate the topographic distribution and attentional modulation of each harmonic in standardized units of signal-to-noise ratio (i.e., controlling for the differences in the overall amplitude and variability between the two harmonics).

*Result 1: Topographic segregation of the 1<sup>st</sup> and 2<sup>nd</sup> harmonics*

SSVEPs were elicited by circular gratings flickered at one of five different frequencies: 6.25, 8.33, 12.5, 16.67, or 25 Hz. Gratings were presented one at a time in the left or right visual hemifield (Figure 2-1). Selection of frequency and hemifield was randomized across trials. Each trial lasted 4.8 s, during which time the observer viewed a flickered grating while maintaining eye fixation at a central marker.

The SSVEPs averaged across all flicker frequencies showed a clear topographic segregation based on response harmonics. The 1<sup>st</sup> harmonic showed a medial posterior localization regardless of whether the grating was located in the left or right visual hemifield (Figure 2-2A, upper row). In contrast, the 2<sup>nd</sup> harmonic showed a clear contralateral posterior localization (Figure 2-2A, lower row).

To statistically evaluate this topographic segregation, we analyzed responses from ten posterior electrodes, five from each cerebral hemisphere (illustrated in Figure 2-2B). These locations correspond to the overall posterior focus of the SSVEPs (Figure 2-2A). The degree of response lateralization was measured as the difference in SSVEP amplitudes between the contralateral and ipsilateral sets of electrodes. Whereas the 1<sup>st</sup> harmonic was similar for the contralateral and ipsilateral electrodes, the 2<sup>nd</sup> harmonic was substantially stronger for the contralateral than for the ipsilateral electrodes (Figure 2-2B). This harmonic-based difference in SSVEP lateralization was confirmed by a significant interaction between the response harmonic

(1<sup>st</sup> vs. 2<sup>nd</sup>) and scalp location (contralateral vs. ipsilateral),  $F_{1,9} = 10.72$ ,  $P < 0.01$ . The overall data (averaged across all flicker frequencies) thus clearly demonstrates a topographic segregation of the 1<sup>st</sup> and 2<sup>nd</sup> harmonics, with the 1<sup>st</sup> harmonic localized to a medial-posterior scalp region and the 2<sup>nd</sup> harmonic localized to a contralateral-posterior scalp region.

We next determined whether the harmonic-based SSVEP lateralization occurred over and above any frequency dependencies of SSVEPs. We quantified the degree of response lateralization as the contralateral minus ipsilateral responses, with a larger positive value indicating stronger contralateral localization and a value near zero indicating no lateralization. The degree of response lateralization for the 1<sup>st</sup> (dashed line) and 2<sup>nd</sup> (solid line) harmonics is plotted as a function of flicker frequency in Figure 2-2C. Note that the response frequencies are twice the flicker frequencies for the 2<sup>nd</sup> harmonics.

It is clear that the 1<sup>st</sup> harmonic was never lateralized across all flicker frequencies. In contrast, lateralization of the 2<sup>nd</sup> harmonic exhibited an inverted U-shaped dependence on frequency. Whereas the 2<sup>nd</sup> harmonic was strongly lateralized for the mid-range response frequencies (16.67 Hz to 33.33 Hz), the lateralization disappeared for the lowest (12.5 Hz) and highest (50 Hz) response frequencies. Note that these harmonic and frequency dependencies of SSVEP lateralization cannot be simply accounted for by the frequency dependence of SSVEP amplitudes. It was not the case that lateralization was weak when the overall response amplitude was weak. Specifically, the overall amplitude of the 2<sup>nd</sup> harmonic monotonically decreased with increasing frequency (Figure 2-2D, right panel), whereas the lateralization (the difference between the solid and dashed curve) disappeared at both the highest and lowest frequencies. The 1<sup>st</sup> harmonic peaked at 8.33 Hz, but there was no lateralization regardless of its amplitude (Figure 2-3B, left panel). Our results thus suggest that the 2<sup>nd</sup> harmonic is selectively lateralized

for the mid-range (16.67 Hz to 33.33 Hz) response frequencies, whereas the 1<sup>st</sup> harmonic is generally non-lateralized.

Finally, we statistically confirmed that the medial versus contralateral segregation of the 1<sup>st</sup> and 2<sup>nd</sup> harmonics are indeed due to differences in harmonics rather than due to differences in absolute frequencies. Within the range of frequencies in which the 2<sup>nd</sup> harmonic was lateralized (Figure 2-2C), both the 1<sup>st</sup> harmonic elicited by the 16.67 Hz flicker and the 2<sup>nd</sup> harmonic elicited by the 8.33 Hz flicker had an identical response frequency of 16.67 Hz, and both the 1<sup>st</sup> harmonic elicited by the 25 Hz flicker and the 2<sup>nd</sup> harmonic elicited by the 12.5 Hz flicker had an identical response frequency of 25 Hz. In both cases, the crucial harmonic (1<sup>st</sup> vs. 2<sup>nd</sup>) by scalp location (contralateral vs. ipsilateral) interactions were significant ( $F_{1,9} = 25.54, P < 0.001$  for 16.67 Hz and  $F_{1,9} = 11.47, P < 0.01$  for 25 Hz), confirming the harmonic-based (rather than frequency-based) topographic segregation of SSVEPs into medial posterior (1<sup>st</sup> harmonic) and contralateral posterior (2<sup>nd</sup> harmonic) scalp regions. Given the relatively coarse spatial resolution of EEG signals, the clear harmonic-based topographic segregation demonstrated here is remarkable, suggesting that the visual system channels the 1<sup>st</sup> and 2<sup>nd</sup> harmonics into well-separated neural assemblies.

### *Result 2: Attentional modulations of the 1<sup>st</sup> and 2<sup>nd</sup> harmonics*

We next examined the possibility that this harmonic-based segregation of population neural activity might reflect an adaptive strategy for resolving conflicting demands in relation to attentional modulations of sensory signals. Whereas the ability to selectively enhance behaviorally relevant aspects of the signals is important, it is also important to preserve undistorted sensory qualities.

We manipulated spatial attention while the observer viewed two circular gratings of different contrasts (one flickering at 16.67 Hz and the other at 12.5 Hz) presented to the left and right visual hemifields (Figure 2-3). The observer voluntarily attended to either the left or right grating while we recorded the SSVEPs elicited by both gratings. The two gratings were flickered at different frequencies (one at 12.5 Hz and the other at 16.67 Hz) so that we could separately monitor the SSVEPs elicited by the attended and ignored gratings based on frequency tagging (the data for the 2<sup>nd</sup> harmonic were reported in Kim et al., 2007). Because the two flicker frequencies produced similar patterns of results with respect to attention effects on the 1<sup>st</sup> and 2<sup>nd</sup> harmonics, we averaged the data from the two frequencies.

We first confirmed that the 1<sup>st</sup> and 2<sup>nd</sup> harmonics were medially and contralaterally localized, respectively, even when two gratings with different flicker frequencies were simultaneously presented (Figure 2-4A). We then compared the attentional modulation of the 1<sup>st</sup> harmonic recorded from the medial posterior electrodes with the attentional modulation of the 2<sup>nd</sup> harmonic recorded from the contralateral posterior electrodes. Voluntary spatial attention selectively boosted the 2<sup>nd</sup> harmonic without affecting the 1<sup>st</sup> harmonic (Figure 2-4B, upper row). This asymmetric effect of attention on the two harmonics was confirmed by the significant harmonic (1<sup>st</sup> vs. 2<sup>nd</sup>) by attention (attended vs. ignored) interaction,  $F_{1,7} = 44.39$ ,  $P < 0.0005$ . Note that prior studies reported attentional modulations of the 1<sup>st</sup> harmonic, using on-off flickered stimuli which primarily generated the 1<sup>st</sup> harmonic (e.g., Müller et al., 1998ab, 2003). Here, using light-dark flickered stimuli which generated robust 2<sup>nd</sup> and 1<sup>st</sup> harmonics, thereby simultaneously measuring attention effects on both harmonics, we have demonstrated that spatial selective attention modulates the 2<sup>nd</sup> harmonic substantially more strongly than it modulates the 1<sup>st</sup> harmonic. Furthermore, the contrast response functions (SSVEP amplitudes as a function of

stimulus contrast) show that, whereas attention multiplicatively boosts the 2<sup>nd</sup> harmonic (Figure 2-4B, lower right panel), undistorted contrast information is simultaneously preserved in the 1<sup>st</sup> harmonic (Figure 2-4B, lower left panel).

*Discussion:*

Dynamic stimuli are typical in our visual environment and they generate complex Fourier spectra in neural responses. To understand the role of temporal structure in visual coding, we examined electrophysiological responses to individual Fourier components using flickered stimuli. We have found evidence that the harmonics of neural responses may form a basis for parallel visual pathways that subservise complementary functions. The first evidence derives from the topographical segregation of the 1<sup>st</sup> and 2<sup>nd</sup> harmonics; whereas the 1<sup>st</sup> harmonic is localized in the medial posterior scalp region, the simultaneously generated 2<sup>nd</sup> harmonic is localized in the contralateral posterior scalp region. Importantly, this topographical segregation is based on response harmonics rather than on absolute response frequencies. Given the relatively coarse spatial resolution of EEG, the robust scalp segregation of the two harmonics (Figures 2-2A and 2-4A) implies a substantial anatomical segregation of the processes mediated by the 1<sup>st</sup> and 2<sup>nd</sup> harmonics.

Prior research has suggested that the 1<sup>st</sup> harmonic originates primarily from the non-frequency-doubling cortical simple cells whereas the 2<sup>nd</sup> harmonic originates primarily from the frequency-doubling cortical complex cells (De Valois et al., 1982; Hubel & Wiesel, 1968; Levitt et al., 1994). However, because distributions of simple and complex cells overlap in the primary visual cortex (e.g., Shapley, 2004), it is unlikely that the topographically segregated 1<sup>st</sup> and 2<sup>nd</sup> harmonics are generated by population responses from simple and complex cells. The lateralized 2<sup>nd</sup> harmonic might still originate from the frequency-doubling complex cells as they provide

primary input to higher-level visual areas such as V4 and MT (e.g., Pollen et al., 2002; Priebe et al., 2006; Cadieu et al., 2007) where the representations of the left and right visual hemifields are substantially more anatomically segregated than they are in the primary visual cortex.

Irrespective of the exact origin of the 1<sup>st</sup> and 2<sup>nd</sup> harmonics, our demonstration of the anatomical segregation of the “1<sup>st</sup>-harmonic-tuned” and “2<sup>nd</sup>-harmonic-tuned” neural processes (clearly detectable with the low spatial resolution of EEG) raises the possibility that complementary visual functions might be mapped onto the two dominant harmonics.

Our attention results suggest these complementary functions are related to the conflicting goals inherent in the attentional control of visual signals. On one hand, substantial attentional modulation of visual processing is desirable to selectively process behaviorally relevant signals. On the other hand, it is also necessary to preserve relatively undistorted sensory signals to correctly encode contrast information. Behavioral results indicate that these goals are generally met in the human visual system; they have demonstrated substantial attentional modulations of stimulus salience and detectability (e.g., Blaser et al., 1999; Simons, 2000; Suzuki, 2003) with relatively modest attentional modulations of perceived contrast (e.g., Carrasco et al., 2004; Prinzmetal et al., 1997). Our result suggests that attentional control of salience is mediated by the 2<sup>nd</sup> harmonic localized in the contralateral posterior scalp region (Figures 2-2A and 2-4A, lower row), which is substantially modulated by top-down influence (Figure 2-4B, lower right panel), whereas preservation of contrast information is mediated by the 1<sup>st</sup> harmonic localized in the medial posterior scalp region (Figures 2-2A and 2-4A, upper row), which carries accurate contrast information relatively undistorted by the variability in the observer’s cognitive state such as level of attention (Figure 2-4B, lower right panel).

Uncovering this division of labor provides a potential resolution to the more than 100-year-old debate as to whether attention affects the intensity of sensation. For example, Fechner strongly denied this possibility, stating that, “gray paper appears to us no lighter, the pendulum-beat of a clock no louder, no matter how much we increase the strain of our attention upon them. No one, by doing this, can make the gray paper look white...” (James, 1890). James (1890), in contrast, asserted that, “attention makes a sense-impression more intense.” To give credit to both Fechner and James, attention may intensify sensation and influence stimulus selection by substantially modulating the 2<sup>nd</sup> harmonic, while simultaneously preserving the accuracy of sensation in the 1<sup>st</sup> harmonic.

#### **4. SYNCHRONIZATION AT BEHAVIORAL LEVEL**

##### **Experiment 3 – Stochastic resonance in binocular rivalry**

Making flexible decisions requires consideration of multiple potential interpretations of a given situation. It is therefore crucial to maintain conscious awareness in a meta-stable state in which each state of awareness is only marginally stable, such that awareness can shift among multiple interpretations compatible with a given stimulus environment. In the visual domain, this translates to dynamic perceptual switching among alternative scene interpretations, for example, seeing “the trees within the forest” and “the forest made up of the trees.” This flexibility is important because behaviorally significant information may exist at different levels of scene organization (e.g., a tiger hidden behind a tree, a layout of the trees indicating a path; see Leopold & Logothetis, 1999, for a discussion of the functional significance of perceptual multistability).

A classic psychophysical paradigm used to study spontaneous perceptual switching is binocular rivalry. When a different image is presented to each eye using a stereoscope, the

perceived image, rather than being a superposition of the two images, tends to spontaneously alternate between them, typically every 0.5-3 s (e.g., Blake, 1989; Logothetis, 1998; Blake, 2001; Blake & Logothetis, 2002). Binocular rivalry can also be multi-stable (involving more than two interpretations; e.g., Suzuki & Grabowecky, 2002a). The observer typically views a rivalrous display continuously, and presses a key corresponding to the visible (dominant) image whenever the percept switches. Data from binocular rivalry thus typically consist of a time series of perceptual-dominance durations for the two competing images. Because the physical stimuli remain constant during binocular rivalry and the dynamics of rivalry are similar whether or not images are stabilized on the retina (e.g., Blake et al., 1971; Wade, 1974), perceptual alternations during binocular rivalry reveal brain mechanisms involved in controlling states of visual awareness.

Spontaneous perceptual alternations in binocular rivalry are thought to result from adaptation and inhibitory interactions occurring at multiple processing stages involving neural populations responsive to different aspects of the competing images. For example, behavioral studies have provided evidence for both eye-based competition (presumably mediated by monocular neurons in V1<sup>1</sup>; e.g., Blake & Fox, 1974; Lack, 1974; Blake et al., 1980; Lee & Blake, 1999) and pattern-based competition (presumably mediated by binocular neurons in higher visual areas; e.g., Logothetis et al., 1996). Human brain imaging (fMRI) studies suggest a prominent role of V1 and/or a prominent role of feedback signals to V1 from higher visual areas (e.g., Polonsky et al., 2000; Tong & Engel, 2001) in resolving perceptual competition. Primate single-cell recording studies (measuring spike rates) found that all-or-none type competition did not occur until inferotemporal cortex while the lower visual areas played intermediate roles (e.g.

---

<sup>1</sup> Eye preferences are also preserved to some degree in higher cortical visual areas (e.g., Gross et al., 1972; see the discussion section of Schröder et al., 2002 for a brief review).

Leopold & Logothetis, 1996; Sheinberg & Logothetis, 1997; Logothetis, 1998).

Electrophysiological studies (e.g., EEG and MEG) have suggested that overall neural activity was stronger and more coherent for a visible image than for a suppressed image during binocular rivalry (e.g., Brown & Norcia, 1997; Tononi et al., 1998; Srinivasan et al., 1999). A full understanding of the intricate multi-stage neural interactions underlying perceptual switching requires a deeper understanding of how neural population activity measured by fMRI, EEG, and MEG are related to single-cell activity (e.g., Hämäläinen et al., 1993; Logothetis, 2003; Vanni et al., 2004).

To tackle perceptual multistability from an implementation perspective, computational models of binocular rivalry have focused on simplified systems that can account for behavioral results to date, aiming to understand the core mechanisms underlying spontaneous perceptual switching. These “macroscopic” models typically involve inhibitory interactions between two pools of neural units preferentially tuned to the competing images (e.g., Sugie, 1982; Lehky, 1988; Blake, 1989; Wilson, 1999). Appropriate implementations of non-linearity in these inhibitory interactions (potentially mediated by spike-frequency adaptation and synaptic depression; e.g., Laing & Chow, 2002) allow a model system to exhibit the mutually exclusive, all-or-none, perceptual switches typically observed in binocular rivalry (e.g., Wilson, 1999). The existing models are successful in generating spontaneous oscillatory behavior and in simulating time-averaged behaviors of binocular rivalry such as how average dominance durations of the competing images depend on their absolute and relative luminance contrasts (e.g., Lehky, 1988; Mueller, 1990; Laing & Chow, 2002; Wilson, 2003). However, these models have not been rigorously tested with respect to their dynamics.

Binocular rivalry as well as other forms of perceptual multistability (e.g., monocular rivalry and figural multistability; see Leopold & Logothetis, 1999, and Blake & Logothetis, 2002 for reviews) exhibit stochastic dynamics; that is, though the time series of perceptual alternations tend to be roughly periodic, the current duration of perceptual dominance cannot be predicted on the basis of the prior dynamics of dominance durations (e.g., lack of autocorrelation, Lathrop values not significantly different from 1, and no evidence of deterministic chaos; e.g., Lathrop, 1966; Fox & Herrmann, 1967; Blake et al., 1971; Borsellino et al., 1972; Taylor & Aldridge, 1974; Richards et al., 1994; Lehky, 1995). Because of these stochastic dynamics, it has been speculated that internal neural noise (in addition to adaptation and inhibitory neural interactions) might play a crucial role in initiating spontaneous perceptual switches (e.g., Sugie, 1982; Lehky, 1988; Haken, 1995; Blake, 2001). Accordingly, random noise was typically added to the activity of the simulated neural units. The dynamic behaviors of the models were then verified by successful fits of the positively skewed frequency distributions of dominance durations obtained from spontaneous binocular rivalry (e.g., Lehky, 1988; Wilson, 1999; Laing & Chow, 2002).

The shapes of spontaneous dominance-duration distributions, however, do not provide adequately rigorous constraints for testing model dynamics; any model that has adaptation, inhibitory interactions, and noise as free parameters can generate appropriately positively skewed dominance-duration distributions. Thus, there is a need for new empirical constraints on the dynamics of binocular rivalry to both distinguish among and improve existing models.

Furthermore, despite the hypothesized role of internal noise in initiating perceptual switches, there has been little evaluation of the nature of this internal neural noise. We thus actively probed the dynamics of perceptual switches using a perturbation technique to determine whether the underlying neural adaptation and inhibitory interactions were coupled with noise in such a way

that the system produced stochastic resonance. As we will discuss later, a demonstration of stochastic resonance in binocular rivalry provides novel dynamic constraints on the existing and future computational models of spontaneous perceptual switching.

The two most prominent features of binocular rivalry, (1) mutually exclusive (non-linear) perceptual switches and (2) the stochastic nature of the time series of the dominance durations, are compatible with a double-well potential framework (e.g., Haken, 1995; Gammaitoni et al., 1998; Suzuki & Grabowecky, 2002a; see Sperling, 1970, for an early theoretical application of a double-well potential framework to the dynamics of binocular fusion, stereopsis, and rivalry). In this framework, the two potential wells correspond to the two alternating, marginally stable percepts. Intuitively, the perceptual state can be considered to be like a ball (depicted with a smiley-face in Figure 3-1) that temporarily gets trapped in one of the two wells. The ball jitters due to random noise, and when the amplitude of the jitter happens to exceed the potential barrier between the two wells, the ball hops to the other well and the percept switches. Thus, greater noise (relative to the height of the potential barrier) should on average produce faster perceptual switches. In addition, neural adaptation and inhibitory interactions could raise the well that has the ball, making the ball more likely to hop to the other well. Thus, stronger adaptation and inhibitory interactions could also increase the switching rate.

All dynamic models of binocular rivalry are overall consistent with a double-well potential framework by virtue of successfully generating two marginally stable states (e.g., Wilson, 1999). However, if the switching between the marginally stable states were generated by a particular type of coupling between neural interactions and noise, spontaneous alternations between the two states could be probabilistically influenced by an applied periodic perturbation that modulates the strengths of the two states (i.e., the depth of the two wells) in opposite phase.

Specifically, a resonance should occur when the frequency of the periodic signal matches the average spontaneous alternation rate of the system (see Gammaitoni et al., 1998, for mathematical derivations). This phenomenon is generally known as stochastic resonance—a noise-mediated cooperative phenomenon in which noise increases sensitivity to a weak periodic signal when the frequency of the periodic signal matches the intrinsic noise-dependent time-scale of the system (e.g., Bulsara et al., 1991; Longtin et al., 1991; Wiesenfeld & Moss, 1995; Gammaitoni et al., 1998).

To determine whether the mechanisms underlying binocular rivalry supported stochastic resonance, we perturbed the relative strength of the two perceptual states by modulating the luminance contrast of the competing stimuli in opposite phase. It is known that the dominance duration is on average longer for the image with higher luminance contrast when other factors such as motion, contour density, and grouping are held constant (see Blake & Logothetis, 2002, for a review). Specifically, increasing and decreasing the contrast of one image primarily decreases and increases, respectively, the dominance duration of the competing image (Levelt's 2<sup>nd</sup> proposition, Levelt, 1965). A longer dominance duration implies a deeper potential well because it takes longer for the perceptual state to hop out of a deeper well than out of a shallower well. Thus, increasing and decreasing the contrast of one image should make the potential well for the competing image shallower and deeper, respectively. Because we varied the contrast of the competing images simultaneously in opposite phase, the depth of the two potential wells should have been modulated in opposite phase. Thus, if adaptation, inhibitory modulations, and noise underlying binocular rivalry interacted in a specific way that satisfied the requirements for stochastic resonance, rivalry should be maximally influenced by a periodic contrast modulation when the modulation frequency matches the average spontaneous rate of perceptual switching.

In previous studies in which stochastic resonance was induced in biological systems (the central and peripheral nervous systems of paddlefish, crayfish, crickets, and humans), an appropriate level of external noise was added to adjust the system's dynamics to match the specific frequency of a weak periodic signal (e.g., Douglass et al., 1993; Levin & Miller, 1996; Cordo et al., 1997; Simonotto et al., 1997; Russell et al., 1999; Mori & Kai, 2002). Theoretically, internal noise should be just as effective as external noise in producing stochastic resonance (e.g., Riani & Simonotto, 1994; Gluckman et al., 1996; Hänggi, 2002). In particular, Riani and Simonotto (1994) reported computer simulation results predicting that the internal neural noise in an appropriate double-well-potential framework could support both spontaneous perceptual switching and stochastic resonance in perception of ambiguous figures. We tested this prediction by attempting to induce internal-noise-based stochastic resonance in the human visual system for mechanisms that control spontaneous perceptual switches in binocular rivalry.

In attempting to induce stochastic resonance in perceptual switching, it is technically difficult to systematically vary the magnitude of the relevant internal neural noise. For example, rapidly and randomly fluctuating the image contrast would not generate corresponding neural noise at the processing stages critical to perceptual switching because binocular rivalry exhibits a wide (several hundred milliseconds) window of temporal summation (O'Shea & Crassini, 1984). Thus, instead of varying the internal noise to adjust the dynamics of spontaneous perceptual switching to match the frequency of a periodic signal, we varied the frequency of a periodic signal to attempt to match the existing internal-noise-based dynamics of perceptual switching.

We first induced clear spontaneous perceptual alternations between a “+” shape and an “x” shape by projecting them to different eyes (using a stereoscope). We then applied periodic signals by modulating the luminance contrasts of the two shapes in opposite phase (i.e., when

one shape was higher contrast, the other shape was lower contrast). This hypothetically corresponds to modulating the depths of the two potential wells, one corresponding to the percept of “+” and other corresponding to the percept of “x,” in opposite phase (see Figure 3-1 and the discussion above). We then predicted that binocular rivalry should exhibit stochastic resonance when the contrast-modulation frequency matched the average rate of spontaneous perceptual switching.

It is important to note that the amplitude of contrast modulation must be appropriately tuned to the magnitude of the internal noise (e.g. Ward, 2002). On the one hand, when the modulation amplitude is substantially lower than the internal noise, the signal is too weak to influence binocular rivalry because perceptual alternations will be predominantly influenced by internal noise; on the other hand, when the modulation amplitude is substantially higher than the internal noise, binocular rivalry will be completely captured by the contrast modulation (e.g., O’Shea & Crassini, 1984). Note that a signal that is too weak to modulate perceptual switching may still be clearly visible (i.e., above sensory threshold). The requirement that the contrast-modulation amplitude must be appropriately tuned to the magnitude of the internal noise for induction of stochastic resonance provides a method to probe the internal noise that influences the dynamics of perceptual switching. Specifically, by finding an appropriate amplitude of contrast modulation that induces stochastic resonance in binocular rivalry, we can estimate the magnitude of the relevant internal noise in terms of the equivalent contrast-modulation amplitude.

If the mechanisms underlying binocular rivalry support stochastic resonance, in addition to the strong resonance that occurs when the signal frequency matches the spontaneous rate of perceptual alternation, higher-order resonance peaks should be observed (when modulation frequencies are appropriate) in the dominance-duration distributions at the odd-integer multiples

of the half-period of contrast modulation. Although the reader is referred to Gammaitoni et al. (1998) for the mathematical derivations, we present the following intuitive description. In our cartoon illustration of an appropriate double-well potential framework shown in Figure 1, the noise is coupled linearly with the periodic signal; in other words, while the depth of the two potential wells oscillate in opposite phase (due to the periodic signal), the noise adds random jitter that probabilistically tosses the state across the middle barrier. The primary peak of the dominance duration distribution should occur exactly at the modulation half-period as a consequence of a tendency for the perceptual state (i.e., the perceived shape) to change in synchrony with the oscillation of the wells (i.e., the changes in the relative contrast of the two shapes) (Figure 3-1A). This primary peak should become predominant at resonance when the contrast-modulation half-period matches the average half-period of spontaneous perceptual switching. A second peak (if any) should occur at 3 times the modulation half-period when perception fails to shift at the first favorable change in the relative contrast, and shifts at the next favorable change (Figure 3-1B). Similarly, a third peak should occur at 5 times the modulation half-period when perception fails to shift at two consecutive favorable changes in contrast, and so on. The higher order peaks should occur with diminishing gains.

To summarize, if the mechanisms underlying perceptual alternations in binocular rivalry are characterized by a particular type of double-well potential landscape and noise that supports stochastic resonance, the relevant differential equations make the following quantitative predictions. When binocular rivalry is subjected to contrast modulation of an amplitude tuned to the magnitude of internal noise, (1) a resonance should occur when the frequency of contrast modulation matches the average spontaneous alternation rate of binocular rivalry, and (2) dominance-duration distributions should exhibit peaks at the odd-integer multiples of the half-

period of contrast modulation. By psychophysically demonstrating these predicted phenomena, we revealed internal-noise-based stochastic resonance in perceptual switching, and provided insights into the nature of the relevant internal noise (its magnitude, locus, and calibration). Furthermore, by evaluating how some representative dynamic models of binocular rivalry are constrained by the current results, we demonstrated the importance and usefulness of the requirement of stochastic resonance in modeling perceptual switching.

*Observers:*

Two psychophysically trained observers, YS and ET, who were naïve to the purpose of the experiments, and author SS, participated.

*Stimuli & procedure:*

A dark “+” shape and a light “x” shape were used as rivaling patterns (see Figure 3-2). They were presented against a gray immediate background ( $70 \text{ cd/m}^2$  in the blink-allowed condition [YS only] or  $46 \text{ cd/m}^2$  in the no-blink condition [all observers]) on a 21” color monitor (75Hz) in a dimly lit room, using Vision Shell software (Micro ML, Inc.). A stereoscope consisting of four front-surface mirrors and a central divider was used to present stimuli dichoptically. To facilitate exclusive binocular rivalry (i.e., clear alternations of “+” and “x” without perception of mixed parts from both shapes), the rivaling patterns were small ( $< 1^\circ$  visual angle), opposite in luminance polarity, consisted of differentially oriented edges, and were presented parafoveally ( $\sim 0.35^\circ$  eccentricity).

All observers were tested in the no-blink condition (no blinking allowed during each continuous stimulus observation). YS was also tested in the blink-allowed condition (natural blinking) to verify that the pattern of results was not influenced by blinking. All the results discussed were equivalent whether or not blinking was allowed.

In each trial in the blink-allowed condition, YS continuously viewed the rivalry display for 60 sec while indicating, by pressing joystick buttons, the perceived shape (“+” or “x”) whenever it changed; in no case were perceptual alternations too rapid to be reported with manual button presses. In the no-blink condition (all observers), each 60 sec run was replaced by a pair of 16 sec runs with a short break in between; trials in which blinking occurred were replaced.

The luminance contrasts of the two shapes were square-wave<sup>2</sup> modulated in opposite phase (i.e., when one shape was higher contrast, the other shape was lower contrast). We defined the higher contrast as the *baseline contrast* because the amplitude of the contrast modulation was always varied by choosing a different value for the lower contrast; we used the usual definition

of image contrast,  $C = \frac{L_{Stimulus} - L_{Background}}{L_{Stimulus} + L_{Background}}$ , where  $L$  indicates luminance.

In the blink-allowed condition (YS only), the baseline contrast,  $C_{Baseline}$ , was always 0.50.

The lower contrast,  $C_{Lower}$ , was chosen such that the percent contrast modulation, defined as

$$\frac{C_{Baseline} - C_{Lower}}{C_{Baseline}} \times 100\%, \text{ was either 40\% or 20\%.}$$

---

<sup>2</sup> We used square-wave rather than sinusoidal contrast modulations partly to keep the impacts of the rising and falling components of the contrast signals constant across different modulation frequencies. Higher harmonics in the square wave (i.e., 3<sup>rd</sup>, 5<sup>th</sup>, 7<sup>th</sup>...) could have produced multiple primary resonances at 3, 5, 7..., times faster than the modulation frequency. These resonances could have shown up in the dominance duration distributions as peaks faster than the primary peak for the fundamental frequency. Such peaks were not evident in the data (see Figure 2) presumably because the amplitudes of the higher harmonics (falling by 1/k for the k<sup>th</sup> harmonic) would have been too small to generate detectable resonance. Furthermore, the higher harmonics would have been irrelevant when the modulation half period was 600 ms or faster because even the 3<sup>rd</sup> harmonic would have had the half period of 200 ms or shorter. This would have been too fast to exert any influence because even when the fundamental had the half period of 200 ms, no corresponding peak occurred (see the lack of resonance peak corresponding to the modulation half period, *HP*, in the rightmost dominance-duration distribution shown in Figure 2). This is important because we obtained evidence of odd-integer multiple peaks in the dominance-duration distributions most strongly for half periods of 400 ms and 600 ms, for which the higher harmonics of the square waves would have made no contributions. Finally, we note that a transient signal presented to one eye can induce dominance of the corresponding stimulus (e.g., Wolfe, 1984). In our design, such transient effects were cancelled out because the contrasts in the two eyes were simultaneously modulated.

In the no-blink condition (all observers), two baseline contrasts,  $C_{Baseline} = 0.50$  and  $C_{Baseline} = 0.25$ , were used to test the possibility that the influence of contrast modulation on binocular rivalry might depend on the percent contrast modulation independently of the baseline contrast. For each baseline contrast, the percent contrast modulation was either 30% (tested for all observers) or 20% (tested for SS and YS).

Due to normal monitor drift over time, the contrasts slightly varied across sessions ( $SD=0.004$ ). The contrast-modulation frequency was constant during each trial.

Each experimental session consisted of a sweep of contrast-modulation frequencies from 0.28 Hz to 2.48 Hz. The frequencies were varied either in the ascending or descending order while the baseline contrast and the amplitude of contrast modulation remained constant. The order of modulation frequency (ascending or descending), the amplitude of modulation, and the baseline contrast were counterbalanced across sessions.

Control data were collected at the beginning and end of each session. In these control trials, the contrast was modulated more slowly than the maximum spontaneous dominance duration (using a half-period = 6 sec for the blink-allowed and a half-period = 8 sec for the no-blink conditions). This procedure was used to measure spontaneous alternation rates while the static image contrasts were matched to the experimental conditions in which contrast-modulation frequencies were varied within the range of spontaneous alternation rates. At least a 2-min break was given between trials, and each session lasted 1-2 hours (typically, not more than one session per day). The 2-min breaks were sufficient to allow the visual system to recover from contrast adaptation from each trial (e.g., Suzuki & Grabowecky, 2004).

Observer YS completed 20 sessions (in 47 days) of the blink-allowed condition (yielding an average number of perceptual alternations,  $\bar{N} = 453$ , for each combination of contrast-

modulation frequency, modulation amplitude, and baseline contrast) and 32 sessions (in 139 days) of the no-blink condition ( $\bar{N}=182$ ); SS completed 32 sessions (in 83 days) of the no-blink condition ( $\bar{N}=246$ ); ET completed 16 sessions (in 80 days) of the no-blink condition ( $\bar{N}=213$ ). The  $\bar{N}$  for YS in the blink-allowed condition was large because of the longer viewing time per trial and the larger number of trials.

*Results:*

Each graph in the lower half of Figure 3-3 shows the dominance-duration distribution when binocular rivalry was subjected to contrast modulation at a given frequency (indicated at the top of Figure 3-3). The data have been averaged across the three observers and the 0.50 and 0.25 baseline contrasts. All characteristics of the data discussed below were present in the individual cases except that the distributions were noisier due to the smaller number of data points. The contrast-modulation amplitude was 30% to 40% of the baseline contrasts, which was within an appropriate range to induce stochastic resonance (a 20% modulation was ineffective; see Figures 3-4 and 3-5).

The leftmost graph shows the spontaneous (control) dominance-duration distribution in the absence of an effective contrast modulation. In the graphs to the right, the dominance-duration distributions are shown for increasing contrast-modulation frequencies. In each graph, the odd-integer multiples of the modulation half-period are indicated by the vertical lines.

It is clear that the peaks in the dominance-duration distributions occurred at the odd-integer multiples of the half-period of contrast modulation. When the contrast modulation was slow (0.28-0.31 Hz), only the primary peak at the modulation half-period was evident and the peak was small. The primary peak grew in size as the modulation frequency was increased toward resonance (at about 0.50 Hz; see Figures 3 and 5). As the modulation frequency was increased

beyond the primary resonance frequency, higher-order peaks began to appear at the odd integer multiples of the modulation half-period (see 0.63-2.48 Hz modulations). In the upper graphs in Figure 3-3, the leftmost control distribution, reflecting spontaneous perceptual alternations, has been subtracted from each distribution to more clearly show the peaks attributable to the periodic contrast modulations.

Note that when the contrast-modulation frequency was 2.48 Hz (the rightmost graph in Figure 3-3), the primary peak at the modulation half-period was missing and the first peak was at three times the modulation half-period. Interestingly, the 2.48 Hz contrast modulation was clearly visible, and attention mechanisms are known to track much faster stimulus alternations, up to 4 Hz or even 10 Hz (see Suzuki & Grabowecky, 2002b for a review). The absence of the primary peak at 2.48 Hz thus suggests that the mechanisms underlying perceptual alternations in binocular rivalry have their own slow time constraints.

The odd-integer multiple peaks characteristic of stochastic resonance were clearly demonstrated in perceptual alternations in binocular rivalry. We next examined the other signature of stochastic resonance, that maximum resonance (i.e., the maximum influence of contrast modulation) should occur when the contrast-modulation frequency matches the average spontaneous rate of perceptual switching. We first examined intuitive evidence of resonance on the basis of a non-monotonic gain as a function of the modulation frequency. We then verified that the resonance frequency followed variations in the average spontaneous alternation rate.

The influence of each contrast-modulation frequency on perceptual switching can be indexed by the size of the induced primary peak in the dominance-duration distribution at the modulation half-period, which is called  $P_I$  (Gammaitoni et al., 1989; 1998). Typically,  $P_I$  is defined as the proportion of the area under the dominance-duration distribution curve within the

range of  $HP \pm HP/2$ , where  $HP$  indicates the modulation half-period.  $P_I$  is plotted as a function of the contrast-modulation frequency for the three observers in the upper panels of Figure 3-4 (solid curves). Because the dominance-duration distributions were peaked even without contrast modulation (see the leftmost graph in Figure 3-3), the corresponding proportions of area of the control distribution (dashed curves) must be subtracted to obtain the gain in  $P_I$  attributable to the periodic contrast modulations (e.g., Giacomelli, et al., 1999). This  $P_I$  gain (the solid curve minus the dashed curve) is shown in the lower panels of Figure 4 as a function of the contrast-modulation frequency. For the 30% and 40% contrast modulations (the primary graphs in Figure 3-4), the presence of resonance is clearly indicated by the fact that the  $P_I$  gain functions were non-monotonic and strongly peaked (e.g., Gammaitoni et al., 1995). In contrast, the evidence of resonance was much reduced (or absent) when the modulation amplitude was 20% (see the inset graphs in Figures 3-4A and 3-4B, showing nearly overlapping  $P_I$  and control functions in the upper panels, and the flattened  $P_I$  gain functions in the lower panels).

Non-monotonic (i.e., peaked)  $P_I$  and  $P_I$  gain functions are intuitively appealing for revealing the presence of resonance. However, they may not be appropriate for estimating resonance frequencies (e.g., Choi et al, 1998). This is partly because  $P_I$  functions and the corresponding control functions peak at similar frequencies (upper panels of Figure 3-4). The peak of a  $P_I$  function might thus be primarily due to the peak of the corresponding control function, and the peak of a  $P_I$  gain function is likely to be distorted around the peak of the control function due to ceiling effects (note  $P_I \leq 1$ ).

To circumvent this problem in estimating the resonance frequency, we used the coefficient of variation ( $CV$ ), a typically used index of resonance, which is the ratio of the standard deviation to the mean of a dominance-duration distribution (e.g., Pikovsky & Kurths, 1997). This index,

also known as the noise-to-signal ratio, is commonly used in neurophysiology to quantify the regularity of neural responses. *CV* is defined independently of the shape of a time-interval distribution, and has been applied to positively skewed distributions such as ours (e.g., Gabbiani & Koch, 1999; Koch, 1999; Dayan & Abbott, 2001). *CV* is particularly useful in cases such as ours where the magnitude of the internal noise is unknown (note that computation of the signal-to-noise ratio, *SNR*, for example, requires knowledge of both the noise magnitude and the signal amplitude). Because a lower *CV* indicates greater periodicity, resonance is indicated by a sharp dip in the *CV* value<sup>3</sup> as a function of the contrast-modulation frequency (Figure 3-5). The modulation frequency corresponding to the bottom of the dip is the resonance frequency. As can be seen in Figure 5, the resonance frequency approximately matched the average spontaneous alternation rate (indicated by the vertical gray bands in Figure 3-5) for all observers and for both 0.50 and 0.25 baseline contrasts. The *CV* resonance dips were evident when the contrast-modulation amplitude was 30% (the primary graphs in Figure 3-5), but they were substantially reduced (or absent) when the modulation amplitude was 20% (the inset graphs in Figure 3-5, shown for observers SS and YS). Thus, the analyses of  $P_I$ ,  $P_I$  gain, and the *CV* resonance dip consistently indicate that 30% and 40% contrast modulations were effective, whereas 20% modulations were too weak for inducing stochastic resonance in the mechanisms that control perceptual alternations in binocular rivalry.

Because the matching of the resonance frequency to the average spontaneous alternation rate is a critical signature of stochastic resonance, we verified this property in greater detail. It is

---

<sup>3</sup> Means and standard deviations of perceptual-dominance durations are substantially affected by the rare occurrences of unusually slow dominance durations. Thus, for each contrast-modulation frequency and baseline contrast for each observer, dominance durations over three standard deviations from the respective means were excluded when computing the *CV*. This resulted in exclusion of less than 2% of the data. Note that the conclusions drawn from the data remain the same even when the longer durations are de-emphasized using a log transform rather than trimming outliers.

known that image alternation rates gradually slow during the course of a continuous observation of binocular rivalry, presumably due to concurrent contrast adaptation (e.g., Lehky, 1995; Suzuki & Grabowecky, 2004). We thus split each trial into the first and second halves and examined those separately. As expected, the alternation rates slowed in the second half-trials; we note that, though the alternation rates gradually slowed within each continuous-viewing trial, the average rates did not slow across trials; apparently, the 2 min. break inserted between trials was sufficient to induce recovery from contrast adaptation (see also Suzuki & Grabowecky, 2004).

The critical prediction was that the resonance frequency (i.e., the contrast-modulation frequency that minimized the CV) should follow this within-trial slowing of the spontaneous alternation rate. Figure 3-6 plots the relationship between the resonance frequency and the average spontaneous alternation rate. Each pair of connected symbols represents the first half-trials (upper right symbol) and the second half-trials (lower left symbol) for each observer under each baseline contrast shown in Figure 3-5. Note that all pairs have positive slopes that lie in the vicinity of the diagonal with a slope of 1, indicating that the resonance frequency followed the within-trial slowing as well as other variations in spontaneous alternation rates due to different baseline contrasts and individual differences.

*Discussion:*

To understand how neural adaptation and inhibitory interactions are coupled with noise to generate spontaneous perceptual alternations in binocular rivalry, we investigated whether the underlying system supported a specific noise-mediated phenomenon known as stochastic resonance. We confirmed this by demonstrating: (1) that the maximum resonance occurred in perceptual switching when the frequency of the applied periodic signal matched the average rate of spontaneous perceptual switching, and (2) that the distribution of perceptual-dominance

durations exhibited multiple resonance peaks at the odd-integer multiples of the half-period of the periodic signal.

### **Constraining computational models**

Existing computational models have been successful in explaining the detailed time-averaged behavior of binocular rivalry (see Laing & Chow, 2002 for a review). In contrast, those models have not been tested rigorously with respect to their dynamic behavior, primarily due to a lack of stringent behavioral constraints on the dynamics of binocular rivalry. The apparently stochastic time series and the Gamma and/or log-normal shape of dominance-duration distributions did not pose rigorous challenges because most models could fit these properties by adding random noise and adjusting the parameters of adaptation and/or inhibitory interactions. Our demonstration of stochastic resonance in binocular rivalry (in particular the characteristic peaks in the dominance-duration distributions at the odd-integer multiples of the contrast-modulation half-period) provides strict dynamic constraints as well as insights into the roles of adaptive and inhibitory neural interactions, internal noise, and a threshold, in generating spontaneous perceptual switching.

To illustrate these points, we examined behaviors of representative models of binocular rivalry that have been developed to simulate the dynamics of perceptual switching. In particular, we contrasted the astable multivibrator model (Lehkey, 1988), based on a Schmitt trigger that exhibits stochastic resonance (e.g., Melnikov, 1993; Gammaitoni et al., 1998), with often-cited winner-take-all models of the type developed by Wilson (Wilson, 1999; 2003; Wilson et al., 2000; 2001) and Mueller (1990). These models basically capture macroscopic aspects of the spiking neuronal network developed by Laing and Chow (2002). Whereas simulating large populations of neurons (as in a spiking neuronal network model) is beyond the scope of this

primarily empirical study, simplified models are suited for deriving analytical inferences. The comparative analyses of the three representative models provide insights into how our empirical results constrain models of the mechanisms underlying perceptual switches in binocular rivalry.

Despite their critical differences, it is assumed in all three models that spontaneous perceptual switching is primarily driven by neural adaptation and inhibitory interactions described by the following differential equation,

$$\tau \frac{dE_A}{dt} = [sign_A] \bullet E_A + f_A(S_A, H_A, I_B) \text{—Eq. 1,}$$

where the two rivaling images are labeled by A and B,  $E_A$  is the activation (or excitation) of the A-unit (preferentially responsive to image A),  $S_A$  is the strength (e.g., contrast) of image A,  $H_A$  is the slow self-adaptation (or habituation) of the A-unit,  $I_B$  is the inhibitory input from the competing B-unit, and  $\tau$  is the time constant of primary adaptation. The dynamics of the B-unit ( $E_B$ ) are given by exchanging the A and B labels.

The three models differ in terms of (1) whether or not adaptation ( $[sign] = -1$ ) and recovery-from-adaptation ( $[sign] = +1$ ) are yoked to perceptual dominance, (2) the exact forms of contrast response, adaptation, and inhibitory interactions—embedded in the  $f_A(S_A, H_A, I_B)$  term, and implementations of perceptual non-linearity (i.e., how the all-or-none perceptual transitions between the competing images are implemented). We compared these representative models (Lehky, 1988; Wilson, 2003, and its predecessors; and Mueller, 1990) in terms of whether or not they could generate stochastic resonance, and how that depended on their specific implementations of adaptation, inhibitory interactions, noise, and/or perceptual non-linearity.

**The astable multivibrator model (Lehky, 1988).** In this model, it is assumed that the state of perceptual dominance determines whether competing neurons adapt or recover from

adaptation. For example, when image A is perceptually dominant, the A-unit adapts (i.e.,  $[sign_A] = -1$ ) while the B-unit recovers from adaptation (i.e.,  $[sign_B] = +1$ ). Influences of self-adaptation, stimulus strength, and inhibitory interactions are all subsumed in the term,  $[sign] \bullet E$ ; thus, the parameters  $H$  (slow self-adaptation),  $S$  (direct stimulus input), and  $I$  (competitive inhibition) are not explicit in this model. In order to implement the contrast modulations of the competing images, we made a simple assumption that increasing the strength of one image has a proportional inhibitory influence on the units responding to the competing image. That is,

$$f_A(S_A, H_A, I_B) = -I_B = -I \bullet \Delta S_B \text{ —Eq. 2,}$$

where  $\Delta S_B$  is a change in the strength of image B (relative to some default value), and  $I$  is a constant that scales stimulus strength to an inhibitory neural influence. The A and B labels can be exchanged to obtain the equation for  $f_B$ .

Except for the added inhibition term, (inhibition of the A-unit from the B-unit) and (inhibition of the B-unit from the A-unit), the formulation is identical to the original astable multivibrator model (Lehky, 1988). Note that increasing (or decreasing) the contrast of image B decreases (or increases) the activity of the A-unit ( $E_A$ ) due to the  $-I \bullet \Delta S_B$  term, while increasing (or decreasing) the contrast of image A decreases (or increases) the activity of the B-unit ( $E_B$ ) due to the  $-I \bullet \Delta S_A$  term. Thus, this modified astable multivibrator model obeys Levelt's 2<sup>nd</sup> proposition (increasing [or decreasing] contrast of one image decreases [or increases] the dominance duration of the other image). As in Lehky (1988), a random-walk noise,  $D \bullet \delta$  ( $D$  is noise intensity and  $\delta$  randomly assumes  $-1$  or  $+1$  at each time update  $t + \Delta t$  [where  $\Delta t \ll \tau$ ])

in our Euler numerical simulation)<sup>4</sup>, is directly added to the differential equations for the neural responses ( $E_A$  and  $E_B$ ) representing the competing stimuli.

The all-or-none characteristic of perceptual switching between the competing images A and B is implemented by a threshold. For example, when image A is perceptually dominant, the A-unit adapts and the B-unit recovers from adaptation. Image A remains dominant until the activity of the A-unit falls to threshold. At that point, image B becomes perceptually dominant.

In simulating our results, we first fit the control condition (e.g., the leftmost distribution in Figure 3-3) using  $\tau$  and  $D$  as the fitting parameters<sup>5</sup>. We then implemented the square-wave contrast modulation as,  $\Delta S(t) = h \cdot SW(f, \phi, t)$ , where  $h$  corresponds to the neurally transduced amplitude<sup>6</sup> of the contrast modulation, and  $SW(f, \phi, t)$  flips between  $-1$  and  $+1$  with a specific frequency  $f$  and phase  $\phi$  ( $180^\circ$  apart for the two images). As shown in Figure 3-7, the astable multivibrator model produces a good fit for both the odd-integer multiple peaks and the relative height of those peaks, with  $h$  used as the only fitting parameter.

---

<sup>4</sup> We used random-walk noise because it was the form of noise used in Lehky (1988). Random-walk noise is a discrete version (i.e., randomly assuming two discrete values without intermediate values) of random noise. The two forms of noise are virtually equivalent for our purposes because the time steps we used for updating noise were orders of magnitude smaller than  $\tau$  and the contrast-modulation frequency (i.e., both forms of noise effectively approached normal distribution in the time scale of perceptual alternations). Furthermore, induction of stochastic resonance should not depend on the form of noise being random-walk or random. We also verified that the use of random noise did not change our results.

<sup>5</sup> To produce good fits to the control distributions with the astable multivibrator model, we let  $\tau$  diminish monotonically starting at the beginning of each dominant percept (this is equivalent to assuming initially accelerated adaptation relative to exponential). This manipulation, however, was not crucial for this model to produce the multiple stochastic-resonance peaks.  $\tau$  was a constant parameter for fitting with Mueller (1990) and Wilson (2003), but these models had more free parameters than the astable multivibrator model to fit the control distributions. We imposed a refractory period (the minimum time required to complete a perceptual switch) to avoid unrealistically rapid perceptual switches and to improve fits for all three models. In the astable multivibrator and Mueller (1990) models, the unit of time is arbitrary. Thus, when we fit these models to the control distributions, we scaled the mean of the simulated data to the mean of the actual data. For all models, we ran 1500-5000 simulated perceptual switches to fit each dominance-duration distribution.

<sup>6</sup> Because the visual system responds strongly to transient changes in luminance, it is possible that the primary influences of contrast modulation occur at the rising and falling edges of the square-wave modulation. Thus, in fine-tuning the fits, we set  $h$  to zero except for a specified duration following the rising and falling transitions of the square-wave; this duration was adjusted to improve the overall fit, but it was kept constant across all contrast modulation frequencies. The implementation of transient responses improved fits in some cases, but it was not critical for producing the odd-integer multiple peaks.

**Winner-take-all model 1 (Wilson, 2003<sup>7</sup>, and its predecessors).** In these models, the [*sign*] factor in Eq. 1 is always  $-1$ ; the primary adaptation factor is thus not yoked to perceptual dominance. Because these models were partly designed to reflect the neurophysiology of the visual system, they use an elaborated form of  $f_A(S_A, H_A, I_B)$ , including implementations of  $H_A$  (self-adaptation),  $S_A$  (direct stimulus input), and  $I_B$  (competitive inhibition). We have,

$$f_A(S_A, H_A, I_B) = \frac{100 \cdot (\max[\{S_A - g \cdot I_B\}, 0])^2}{(10 + H_A)^2 + (\max[\{S_A - g \cdot I_B\}, 0])^2} \text{---Eq. 3,}$$

$$\tau_I \frac{dI_B}{dt} = -I_B + E_B \text{---Eq. 4,}$$

$$\tau_H \frac{dH_A}{dt} = -H_A + b \cdot E_A \text{---Eq. 5,}$$

where  $\tau_I$  and  $\tau_H$  are the time constants of inhibitory interactions and slow self-adaptation, respectively, and  $\max[X, Y]$  returns the larger of the two values, X and Y. The A and B labels can be exchanged to obtain the equation for  $f_B$ . Levelt's 2<sup>nd</sup> proposition is obeyed because of the competitive inhibition term,  $I_B$ .

The all-or-none characteristic of perceptual switching is implemented by a winner-take-all rule. Perceptual dominance is determined by the relative strength of the A-unit and B-unit; that is, image A is perceptually dominant when  $E_A > E_B$  and image B is perceptually dominant when  $E_B > E_A$ .

As with the astable multivibrator model, we added noise directly to the differential equations for  $E_A$  and  $E_B$ . Because perceptual dominance is determined by the relative activity of

---

<sup>7</sup> We used only the 1<sup>st</sup> stage of the model; the 2<sup>nd</sup> stage would have been redundant because the pattern presented to each eye was constant in our study.

$E_A$  and  $E_B$  (the neural units responding to the competing stimuli), fluctuations in their activity seem to be the natural locus of the relevant noise influencing perceptual switches.

We first fit the baseline conditions using  $S_A, S_B, I, H, b, g$  and  $D$  as the free parameters. We then implemented the square-wave contrast modulation as

$S(t) = S + h \cdot SW(f, \phi, t)$ , where  $S$  is the baseline contrast and  $h$  is the contrast-modulation amplitude. As with the astable multivibrator model, we used  $h$  as the free parameter to fit the odd-integer multiple peaks. We were unable to obtain the primary or higher-order stochastic resonance peaks. Nor were we able to obtain the asymptotic behavior, that is, we were unable to obtain the strong peak expected at the contrast-modulation half period when the amplitude of the modulation was 100% (i.e., presenting the left-eye and right-eye images sequentially).

Note that, in Wilson's model, the locus of noise could be other than the responses of the competing neural units. We verified that this model could simulate Gamma-like spontaneous dominance-duration distributions whether the noise was added to the responses of the competing neural units (i.e., to the differential equations for  $E_A$  and  $E_B$  —Eq. 1), to adaptation of these units (i.e., to the differential equations for  $H_A$  and  $H_B$  —Eq. 5), or to their inhibitory interactions (i.e., to the differential equations for  $I_A$  and  $I_B$  —Eq. 4). Wilson's model simulated our data well when the noise was added to the *adaptation* equations. Adding noise to the inhibitory-interaction equations also produced some of the resonance peaks and the asymptotic behavior, but the quality of fit was inferior (e.g., we failed to produce more than two resonance peaks).

Furthermore, although adding noise to the adaptation equations for  $H$  (affecting the speed of adaptation) produced good fits to our data, adding noise directly to the  $H$  term in Eq. 3 (affecting the impact of adaptation) failed to produce the resonance peaks or the asymptotic behavior. Thus,

if Wilson's model captured the underlying mechanisms of perceptual switching, the noise must primarily affect the speed of adaptation of the competing neural units.

**Winner-take-all model 2 (Mueller, 1990).** This model is overall similar to Wilson (2003) with differences in the forms of the contrast-response function (logarithmic rather than Naka-Rushton) and inhibitory interactions:

$$f_A(S_A, H_A, I_B) = \ln(S_A) - a_A \left( 1 - c_A \frac{\ln(S_A)}{\ln(100)} \right) \bullet I_B - H_A \text{ ---Eq. 9,}$$

$$I_B = \max[E_B, 0] \text{ ---Eq. 10,}$$

$$\tau_H \frac{dH_A}{dt} = H_A + b \bullet \max[E_A, 0] \text{ ---Eq. 11,}$$

where  $\max[X, Y]$  returns the larger of the two values, X and Y. The A and B labels can be exchanged to obtain the equation for  $f_B$ . Levelt's 2<sup>nd</sup> proposition is obeyed because of the competitive inhibition term,  $I_B$ , which is directly proportional to activation of the competing B-unit.

As with Wilson (2003), the all-or-none characteristic of perceptual switching between the competing images A and B is implemented by a winner-take-all rule (i.e., image A is perceptually dominant when  $E_A > E_B$  and image B is perceptually dominant when  $E_B > E_A$ ).

We first fit the baseline conditions using  $S_A, S_B, T, a_A, a_B, b, c_A, c_B$  and  $D$  as free parameters (note that  $S_A = S_B, a_A = a_B,$  and  $c_A = c_B$  as in Mueller, 1990), and then implemented the square-wave contrast modulation as  $S(t) = S + h \bullet SW(f, \phi, t)$ . The simulation results were similar to those for Wilson (2003). When the noise was added to the differential equations for the neural responses, we were unable to obtain the resonance peaks or the asymptotic behavior.

When the noise was added to the differential equations for adaptation (Eq. 11), we were then able to fit the data well.

In summary, while all three dynamic models of perceptual switching are consistent with Levelt's 2<sup>nd</sup> proposition and the general double-well-potential framework, and they can simulate Gamma-shaped dominance duration distributions from spontaneous binocular rivalry, our stochastic resonance results provide additional insights into their implementations of noise and all-or-none perceptual switching. The success of the astable multivibrator model (Lehky, 1988) suggests that the mechanisms underlying perceptual switches might be characterized by simple linear interactions among stimulus input, adaptation, inhibitory modulations, and response noise of the competing neural units, with threshold crossing being the source of all-or-none perceptual switching<sup>8</sup>. Alternatively, our simulation results with Wilson's (2003) and Mueller's (1990) models suggest that if the mechanisms of perceptual switches are characterized by a winner-take-all algorithm coupled with the non-linear interactions among stimulus input, adaptation, and inhibitory modulations implemented in these models, the locus of the critical noise must be in the speed of adaptation rather than in the responses of the competing neural units. Future neurophysiological research might resolve these alternatives by investigating (1) whether perceptual switches are initiated by the reduction to threshold of the activity of the neural units responding to the currently perceptually dominant image or by changes in the sign of the relative activity of the competing units, and (2) whether the rate of perceptual switches is primarily influenced by the response noise in the competing neural units or by fluctuations in the speeds of their adaptation.

---

<sup>8</sup> We verified the importance of threshold crossing in the astable multivibrator model by demonstrating that the model failed to produce the resonance peaks (except for the primary peak) when the algorithm for perceptual switching was changed from threshold-crossing to winner-take all.

### Estimating the internal noise influencing perceptual switching.

Our results also provide insights into the nature of the internal noise that contributes to perceptual switching. In particular, the magnitude of resonance (i.e., the size of the *CV* dips shown in Figure 3-5) depended on the relative rather than the absolute amplitude of contrast modulation. In all of the experiments reported here, the contrast was modulated between the baseline contrast and a reduced contrast. If we define the percent contrast modulation as,

$$\text{Percent contrast modulation} = \frac{[\text{baseline contrast}] - [\text{lower contrast}]}{[\text{baseline contrast}]} \times 100\%,$$

contrast modulations of 30% to 40% clearly produced resonance (see the primary graphs in Figures 3-4 and 3-5), whereas the  $P_I$ ,  $P_I$  gain, and resonance dips were all weak or absent with 20% modulation (see the inset graphs in Figures 3-4 and 3-5).

Two points are noteworthy. First, both 30% and 20% contrast modulations were clearly visible, suggesting that both levels of contrast modulation were above threshold, that is, they were greater than the sensory noise that limits detectability of contrast modulation. This in turn suggests that the system that controls perceptual switching in binocular rivalry has its own noise and threshold which are greater than the sensory noise and threshold that control the visibility of contrast modulations. The fact that 30% contrast modulation clearly produced stochastic resonance but 20% modulation did not, also provides a signal-based estimate of the magnitude of the relevant internal noise, equivalent to somewhere between 20% and 30% of contrast modulation.

Second, the strength of resonance (i.e., the size of resonance dip) was similar for rather different *baseline* contrasts, 0.50 and 0.25, as long as the *percent contrast modulation* was the same (Figure 3-5). We subsequently verified this ratio-wise (divisive) normalization of the

perceptual-switching mechanisms to these baseline contrasts for a wide range of contrast-modulation amplitudes (0%-100%). Thus, internal noise, threshold, and gain of the contrast modulation appear to be calibrated to the baseline contrast in such a way that the mechanisms underlying perceptual switches respond to the proportion of contrast modulation (at least when different baseline contrasts are blocked, allowing time for the visual system to adapt to the baseline contrast).

### **Summary**

We have demonstrated internal-noise based stochastic resonance in binocular rivalry by applying weak periodic contrast modulations to the competing images. Spontaneous perceptual switches in binocular rivalry have been thought to be mediated by interactions among stimulus input, neural adaptation, mutual inhibition, and noise that together generate competing marginally stable states consistent with a double-well potential framework. Our results have shown that these interactions must occur in such a way that the system supports stochastic resonance. Our computational simulations have shown how this stochastic-resonance requirement constrains the current dynamic models of binocular rivalry in terms of the locus of the relevant noise and the algorithm of perceptual switching. The results also suggest that the magnitude of the internal noise involved in perceptual switches is equivalent to approximately 20%-30% of contrast modulation, and that the locus of this noise is beyond the processing stage where sensory noise influences pattern detection. Because the noise magnitude appears to calibrate to baseline contrast, it is possible that the magnitude of internal noise might be adaptively maintained in the brain such that it is low enough to prevent hyper-sensitive responses to small fluctuations in the environment (thus providing sufficient time and stability to analyze

each perceptual interpretation), but high enough to keep the system from getting mired in a single state.

## 5. CONCLUSION

This dissertation has presented evidence that concepts and theories of synchronization are useful to further understanding of the state of the human brain during processing incoming information from our dynamic sensory environment.

In particular, we monitored frequency-tagged steady-state visual evoked potentials (SSVEPs) in humans and found that voluntary sustained attention multiplicatively increased the stimulus-driven population electrophysiological activity. Analyses of inter-trial phase coherence showed that this attentional response gain was at least partially due to increased synchronization of SSVEPs to stimulus flicker. These results suggest that attention operates in a complementary manner at different levels; attention appears to increase single-neuron spike rates in a variety of ways including contrast, response, and activity gain, while also inducing a multiplicative boost on neural population activity via enhanced response synchronization.

It was also discovered that flickered stimuli generated SSVEPs which typically include Fourier components at the flicker frequency (the 1<sup>st</sup> harmonic) and twice the flicker frequency (the 2<sup>nd</sup> harmonic). Our results suggest that these harmonics mediate parallel processing that subserves complementary functions. The 1<sup>st</sup> and 2<sup>nd</sup> harmonics exhibited clearly divergent posterior scalp topography for a broad range of frequencies, with the 1<sup>st</sup> harmonic medially maximal and the 2<sup>nd</sup> harmonic contralaterally maximal. Furthermore, voluntary visual attention modulated the 2<sup>nd</sup> harmonic substantially more strongly than the 1<sup>st</sup> harmonic. These results suggest that the visual system may primarily use frequency-doubled signals for top-down modulations while simultaneously preserving relatively undistorted sensory qualities in the 1<sup>st</sup>

harmonic. This harmonic-based topographic difference might be due to the formation of synchronous clusters where one cluster prefers 1:1 synchronization (the 1<sup>st</sup> harmonic) and another cluster prefers 1:2 synchronization (the 2<sup>nd</sup> harmonic).

Moreover, we demonstrated quantitative evidence of stochastic resonance in binocular rivalry by subjecting binocular rivalry to weak periodic contrast modulations spanning a range of frequencies. Our behavioral results combined with computational simulations provided insights into the nature of the internal noise (its magnitude, locus, and calibration) that is relevant to perceptual switching, as well as provided novel dynamic constraints on computational models designed to capture the neural mechanisms underlying perceptual switching.

All of these findings may find a unifying explanation within a mechanism of synchronization in nonlinear dynamical systems, which may be a general organizing principle of great importance for cognitive processes and account for how we perceive and react to the outside world.

## REFERENCES

- Andronov, A. A., Vitt, E. A., & Khaikin, S. E. (1966). Theory of oscillations. *Pergamon Press*, Oxford.
- Anishchenko, V. S., Astakhov, V. V., Neiman, A. B., Vadivasova, T. E., & Schimansky-Geier, L. (2003). Nonlinear dynamics of chaotic and stochastic systems: Tutorial and modern developments. *Springer-Verlag*, Berlin.
- Azouz, R. & Gray, C. M. (2000). Dynamic spike threshold reveals a mechanism for synaptic coincidence detection in cortical neurons in vivo. *Proceedings of the National Academy of Sciences USA*, 97, 8110-8115.
- Blake, R. (1989). A neural theory of binocular rivalry. *Psychological Review*, 96, 145-167.
- Blake, R. (2001). A primer on binocular rivalry, including current controversies. *Brain and Mind*, 2, 5-38.
- Blake, R. & Fox, R. (1974). Binocular rivalry suppression: insensitive to spatial frequency and orientation change. *Vision Research*, 14, 687-692.
- Blake, R., Fox, R. & McIntyre, C. (1971). Stochastic properties of stabilized-image binocular rivalry alternations. *Journal of Experimental Psychology*, 88, 327-332.
- Blake, R. & Logothetis, N. K. (2002). Visual competition. *Nature Neuroscience*, 3, 1-11.
- Blake, R., Westendorf, D. H., & Overton, R. (1980). What is suppressed during binocular rivalry? *Perception*, 9, 223-231.
- Borsellino, A., De Marco, A., Allazetta, A., Rinesi, S. & Bartolini, B. (1972). Reversal time distribution in the perception of visual ambiguous stimuli. *Kybernetik* 10, 139-144.
- Brown, R. J., & Norcia, A. M. (1997). A method for investigating binocular rivalry in real-time with the steady-state VEP. *Vision Research*, 37(170), 2401-2408.
- Buia, C. & Tiesinga, P. (2006). Attentional modulation of firing rate and synchrony in a model cortical network. *Journal of Computational Neuroscience*, 20, 247-264.
- Buschman, T. J., and Miller, E. K. (2007) Top-down versus bottom-up control of attention in the prefrontal and posterior parietal cortices. *Science*, 315, 1860-1862.
- Bulsara, A., Jacobs, E. W., Zhou, T., Moss, F. & Kiss, L. (1991). Stochastic resonance in a single neuron model: theory and analog simulation. *Journal of Theoretical Biology*, 152(4), 531-55.
- Buzsáki, G. & Draguhn, A. (2004). Neuronal oscillations in cortical networks. *Science*, 304, 1926-1929.
- Cameron, E. L., Tai, J. C., & Carrasco, M. (2002). Covert attention affects the psychometric function of contrast sensitivity. *Vision Research*, 42, 949-967.
- Campbell, F. W. & Maffei, L. (1970). Electrophysiological evidence for the existence of orientation and size detectors in the human visual system. *Journal of Physiology (London)*, 207, 635-652.
- Canolty, R. T., Edwards, E., Dalal, S. S., Soltani, M., Nagarajan, S. S. Kirsch, H. E., Berger, M. S., Barbaro, N. M. & Knight, R. T. (2006). High gamma power is phase-locked to theta oscillations in human neocortex. *Science*, 313, 1626-1628.
- Carrasco, M., Ling, S., & Read, S. (2004). Attention alters appearance. *Nature Neuroscience*, 7, 308-313.

- Chelazzi, L., Duncan, J., Miller, E. K., & Desimone, R. (1998). Responses of neurons in inferior temporal cortex during memory-guided visual search. *Journal of Neurophysiology*, 80, 2918-2940.
- Choi, M.H., Fox, R.F., & Jung, P. (1998). Quantifying stochastic resonance in bistable systems: Response vs. residence-time distributions. *Physical Review E*, 57, 6335-6344.
- Cordo, P., Inglis, J. T., Verschueren, S., Collins, J. J., Merfeld, D.M., Rosenblum, S., Buckley, S. & Moss, F. (1997). Noise in human muscle spindles. *Nature* 383, 769-770.
- Dayan, P. & Abbott, L. F. (2001). *Theoretical Neuroscience: Computational and Mathematical Modeling of Neural Systems*. MIT Press: Cambridge, MA; London, England.
- Delorme, A. & Makeig, S. EEGLAB: an open source toolbox for analysis of single-trial EEG dynamics including independent component analysis. *Journal of Neuroscience Methods*, 134, 9-21.
- Desimone, R., & Duncan, J. (1995). Neural mechanisms of selective visual attention. *Annual Review of Neuroscience*, 18, 193-222.
- De Valois, R. L., Albrecht, D. G. & Thorell, L. G. (1982). Spatial frequency selectivity of cells in macaque visual cortex. *Vision Research* 22, 545-559.
- Ding, J., Sperling, G., & Srinivasan, R. (2005). Attentional modulation of SSVEP power depends on the network tagged by the flicker frequency. *Cerebral Cortex*, 16, 1016-1029.
- Di Russo, F., Spinelli, D., & Morrone, M. C. (2001). Automatic gain control contrast mechanisms are modulated by attention in humans: evidence from visual evoked potentials. *Vision Research*, 41, 2435-2447.
- Di Russo, F., Pitzalis, S., Aprile, T., Spitoni, G., Patria, F., Stella, A., Spinelli, D., & Hillyard, S. A. (2007). Spatiotemporal analysis of the cortical sources of the steady-state visual evoked potential. *Human Brain Mapping* 28(4), 323-334.
- Dougllass, J. K., Wilkens, L., Pantazelou, E. & Moss, F. (1993). Noise enhancement of information transfer in crayfish mechanoreceptors by stochastic resonance. *Nature*, 365, 337-340.
- Edwards, D. P., Purpura, K. P., & Kaplan, E. (1995). Contrast sensitivity and spatial frequency response of primate cortical neurons in and around the cytochrome oxidase blobs. *Vision Research*, 35, 1501-1523.
- Engel, A. K. & Singer, W. (2001). Temporal binding and the neural correlate of sensory awareness. *Trends in Cognitive Sciences*, 5(1), 16-25.
- Engel, A.K., Fries, P., & Singer, W. (2001). Dynamic predictions: oscillations and synchrony in top-down processing. *Nature Reviews Neuroscience*, 2, 704-716.
- Fell, J., Frenandez, G., Klaver, P., Elger, C. E., & Fries, P. (2003). Is synchronized neuronal gamma activity relevant for selective attention? *Brain Research Reviews*, 42, 265-272.
- Femat, R., & Solis-Perales, G. (1999). On the chaos synchronization phenomena. *Physics letters A*. 262(1), 50-60.
- Fox, R. & Herrmann, J. (1967). Stochastic properties of binocular alternations. *Perception & Psychophysics*, 2, 432-436.
- Fries, P., Reynolds, J. H., Rorie, A. E., & Desimone, R. (2001). Modulation of oscillatory neuronal synchronization by selective visual attention. *Science*, 291, 1560-1563.
- Fries, P. (2005). A mechanism for cognitive dynamics: neuronal communication through neuronal coherence. *Trends in Cognitive Sciences*, 9(10), 474-480.

- Fujisaka, H., & Yamada, T. (1983). Stability of synchronized motion in coupled-oscillator systems. *Progress of theoretical physics*, 69(1), 32-47.
- Gabbiani, F. & Koch, C. (1999). Principles of Spike Train Analysis. In C. Koch & I. Segev (Eds.) *Methods in Neural Modeling* (pp.313-360), MIT Press: Cambridge, MA.
- Gammaitoni, L., Hanggi, P., Jung, P. & Marchesoni, F. (1998). Stochastic resonance. *Reviews of Modern Physics*, 70, 223-287.
- Gammaitoni, L., Marchesoni, F., Menichiella-Saetta, E. & Santuci, S. (1989). Stochastic Resonance in Bistable Systems. *Physical Review Letters*, 62, 349-352.
- Gammaitoni, L., Marchesoni, F. & Santuci, S. (1995). Stochastic Resonance as a *Bona Fide* Resonance. *Physical Review Letters*, 74, 1052-1055.
- Geisler, W. S. & Albrecht, D. G. (1997). Visual cortex neurons in monkeys and cats: detection, discrimination, and identification. *Visual Neuroscience*, 14, 897-919.
- Giacomelli, G. Marin, F. & Rabbiaosi, I. (1999). Stochastic and *Bona Fide* Resonance: An Experimental Investigation. *Physical Review Letters*, 82(4) 675-678.
- Gluckman, B. J., Netoff, T. I., Neel, E. J., Ditto, W. L., Spano, M. & Schiff, S. J. (1996). Stochastic Resonance in a Neuronal Network from Mammalian Brain. *Physical Review Letters*, 77, 4098-4101.
- Goodale, M. A., Milner, A. D., Jakobson, L. S., & Carey, D. P. (1991). A neurological dissociation between perceiving objects and grasping them. *Nature*, 349, 154-156.
- Goodale, M. A., & Westwood, D. A. (2004). An evolving view of duplex vision: separate but interacting cortical pathways for perception and action. *Current Opinion in Neurobiology*, 14, 203-211.
- Gray, C. M., Konig, P., Engel, A. K., & Singer, W. (1989). Oscillatory responses in cat visual cortex exhibit inter-columnar synchronization which reflects global stimulus properties. *Nature*, 338, 334-337.
- Grill-Spector, K., & Malach, R. (2004). The human visual cortex. *Annual Review of Neuroscience*, 27, 649-677.
- Gross, C. G., Rocha-Miranda, C. E., & Bender, D. B. (1972). Visual properties of neurons in inferotemporal cortex of the macaque. *Journal of Neurophysiology*, 35, 96-111.
- Guckenheimer, J., & Holmes, P. (1983). Nonlinear oscillations, dynamical systems, and bifurcations of vector fields. *Springer-Verlag*, New York.
- Hänggi, P. (2002). Stochastic resonance in biology. *ChemPhysChem*, 3, 285.
- Haenny, P. E. & Schiller, P. H. (1988). State dependent activity in monkey visual cortex. I. Single cell activity in V1 and V4 on visual tasks. *Experimental Brain Research*, 69, 225-244.
- Haken, H. (1995). Some basic concepts of synergetics with respect to multistability in perception, phase transitions and formation of meaning. In P. Kruse & M. Stadler (Eds.) *Ambiguity in Mind and Nature* (pp.23-43), Springer-Verlag New York.
- Hämäläinen, M., Hari, R., Ilmoniemi, R., Knuutila, J., & Lounasmaa, O. V. (1993). Magnetoencephalography—theory, instrumentation, and applications to noninvasive studies of the working human brain. *Reviews of Modern Physics*, 65, 413-497.
- Hawken, M. J., Shapley, R. M., & Grosz, D. H. (1996). Temporal-frequency sensitivity in monkey visual cortex. *Visual Neuroscience*, 13, 477-492.
- Hayashi, C. (1964). *Nonlinear oscillations in physical systems*. McGraw-Hill, NY.

- Henrie, J. A. & Shapley, R. (2005). LFP power spectra in V1 cortex: the graded effect of stimulus contrast. *Journal of Neurophysiology*, 94, 479-490.
- Hermann, C. S. (2001). Human EEG responses to 1-100 Hz flicker: resonance phenomena in visual cortex and their potential correlation to cognitive phenomena. *Experimental Brain Research*, 137, 346-353.
- Hou, C., Pettet, M. W., Sampath, V., Candy, T. R., & Norcia, A. M. (2003). Development of the spatial organization and dynamics of lateral interactions in the human visual system. *Journal of Neuroscience*, 23, 8630-8640.
- Hubel, D. H. & Wiesel, T. N. (1968). Receptive fields and functional architecture of monkey striate cortex. *Journal of Physiology* 195, 215-243.
- Huang, L. & Dobkins, K. R. (2005). Attentional effects on contrast discrimination in humans: evidence for both contrast gain and response gain. *Vision Research*, 45, 1201-1212.
- Huygens (Hugenii), C. (1673). *Horologium Oscillatorium*. Apud F. Muguet, Parisiis, France.
- James, W. (1890). *The principles of psychology*. New York: Henry Holt.
- Kastner, S., & Ungerleider, L. G. (2000). Mechanisms of visual attention in the human cortex. *Annual Review of Neuroscience*, 23, 315-341.
- Kastner, S., & Ungerleider, L. G. (2001). The neural basis of biased attention in human visual cortex. *Neuropsychologia*, 39, 1263-1276.
- Kim, Y.-J., Grabowecky, M., & Suzuki, S. (2006). Stochastic resonance in binocular rivalry. *Vision Research*, 46, 392-406.
- Kim, Y.-J., Grabowecky, M., Paller, K. A., Muthu, K., & Suzuki, S. (2007). Attention induces synchronization-based response gain in steady-state visual evoked potentials. *Nature neuroscience*. 10, 117-125.
- Kim, Y.-J., Grabowecky, M., Paller, K. A., & Suzuki, S. (2008). Parallel visual processing revealed by evoked oscillatory neural harmonics. *To be submitted*.
- Knight, R. T. (2007). Neural networks debunk phrenology. *Science*. 316, 1578-1579.
- Koch, C. (1999). *Biophysics of Computation: Information Processing in Single Neurons*. Oxford University Press: Oxford.
- Lack, L. C. (1974). Selective attention and the control of binocular rivalry. *Perception & Psychophysics*, 15(1), 193-200.
- Laing, C. R. & Chow, C. C. (2002). A spiking neuron model for binocular rivalry. *Journal of Computational Neuroscience*, 12, 39-53.
- Lathrop, R. G. (1966). First-order response dependencies at a differential brightness threshold. *Journal of Experimental Psychology*, 72, 120-124.
- Lee, D. K., Itti, L., Koch, C., & Braun, J. (1999). Attention activates winner-take-all competition among visual filters. *Nature Neuroscience*, 2, 375-381.
- Lee, S.-H. & Blake, R. (1999). Rival ideas about binocular rivalry. *Vision Research*, 39, 1447-1454.
- Lehky, S. R. (1988) An astable multivibrator model of binocular rivalry. *Perception*, 17, 215-228.
- Lehky, S. R. (1995). Binocular rivalry is not chaotic. *Proceedings of the Royal Society of London B: Biological Sciences*, 259, 71-76.
- Leopold, D. A. & Logothetis, N. K. (1996). Activity changes in early visual cortex reflect monkey's percepts during binocular rivalry. *Nature*, 379, 549-553.

- Leopold, D. A. & Logothetis, N. K. (1999). Multistable phenomena: changing views in perception. *Trends in Cognitive Sciences*, 3, 254-264.
- Levelt, W. J. M. (1965). On Binocular Rivalry (Soesterberg, The Netherlands: Institute for Perception RVO-TNO).
- Levin, J. E. & Miller, J. P. (1996). Broadband neural encoding in the cricket cercal sensory system enhanced by stochastic resonance. *Nature*, 380, 165-168.
- Levitt, J. B., Kiper, D. C. & Movshon, J. A. (1994). Receptive fields and functional architecture of macaque V2. *Journal of Neurophysiology* 71, 2517-2542.
- Ling, S. & Carrasco, M. (2006). Sustained and transient covert attention enhance the signal via different contrast response functions. *Vision Research*, 46, 1210-1220.
- Logothetis, N.K. (1998). Single units and conscious vision. *Philosophical Transactions of the Royal Society of London B: Biological Sciences*, 353, 1801-1818.
- Logothetis, N. K. (2003). The underpinnings of the BOLD functional magnetic resonance imaging signal. *Journal of Neuroscience*, 23(10), 3963-3971.
- Logothetis, N. K., Leopold, D. A., & Sheinberg, D. L. (1996). What is rivaling during binocular rivalry? *Nature*, 380, 621-624.
- Longtin, A., Bulsara, A. & Moss, F. (1991). Time-interval sequences in bistable systems and the noise-induced transmission of information by sensory neurons. *Physical Review Letters*, 67, 656-659.
- Luck, S. J., Hillyard, S. A. Mouloua, M., Woldorff, M. G., Clark, V. P., & Hawkins, H. L. (1994). Effects of spatial cuing on luminance detectability: psychophysical and electrophysiological evidence for early selection. *Journal of Experimental Psychology: Human Perception and Performance*, 20(4), 887-904.
- Martinez-Conde, S., Macknik, S. L., & Hubel, D. H. (2004). The role of fixational eye movements in visual perception. *Nature Reviews Neuroscience*, 5, 229-240.
- Martinez-Trujillo, J. & Treue, S. (2002). Attentional modulation strength in cortical area MT depends on stimulus contrast. *Neuron*, 35, 365-370.
- Maunsell, J. H. & Cook, E. P. (2002). The role of attention in visual processing. *Philosophical Transactions of the Royal Society of London B*, 357, 1063-1072.
- Maunsell, J. H. R., & Treue, S. (2006). Feature-based attention in visual cortex. *Trends in Neurosciences*, 29(6), 317-322.
- Melnikov, V. I. (1993). Schmitt trigger: A solvable model of stochastic resonance. *Physical Review E*, 48, 2481-2489.
- Merigan, W. H. & Maunsell, J. H. R. (1993). How parallel are the primate visual pathways? *Annual Review of Neuroscience*, 16, 369-402.
- Mishkin, M., Ungerleider, L. G., & Macko, K. A. (1983). Object vision and spatial vision: Two central pathways. *Trends in Neuroscience*, 6, 414-417.
- Morgan, S. T., Hansen, J. C. & Hillyard, S. A. (1996). Selective attention to stimulus location modulates the steady-state visual evoked potential. *Proceedings of the National Academy of Sciences of the United States of America*, 93, 4770-4.
- Mori, T. & Kai, S. (2002). Noise-induced entrainment and stochastic resonance in human brain waves. *Physical Review Letters*, 88, 218101/1-4.
- Morrone, M. C., Denti, V., & Spinelli, D. (2002). Color and luminance contrasts attract independent attention. *Current Biology*, 12, 1134-1137.

- Motter, B. C. (1993). Focal attention produces spatially selective processing in visual cortical areas V1, V2, and V4 in the presence of competing stimuli. *Journal of Neurophysiology*, 70, 909-919.
- Mueller, T. J. (1990). A physiological model of binocular rivalry. *Visual Neuroscience*, 4, 63-73.
- Müller, M. M. et al. (1998a). Effects of spatial selective attention on the steady-state visual evoked potential in the 20-28 Hz range. *Cognitive Brain Research* 6, 249-261.
- Müller, M. M., Teder-Sälejärvi, W. & Hillyard, S. A. (1998b). The time course of cortical facilitation during cued shifts of spatial attention. *Nature neuroscience* 1, 631-634.
- Müller, M. M., Malinowski, P., Gruber, T. & Hillyard, S. A. (2003). Sustained division of the attentional spotlight. *Nature* 424, 309-312.
- Neiman, A., Silchenko, A., Anishchenko, V. S., & Schimansky-Geier, L. (1998). Stochastic resonance: Noise-enhanced phase coherence. *Physical Review E*, 58(6), 7118-7125.
- Neiman, A., Pei, X., Russell, D. F., Wojtenek, W., Wilkens, L., Moss, F., Braun, H. A., Huber, M. T., & Voigt, K. (1999a). Synchronization of the noisy electrosensitive cells in the paddlefish. *Physical Review Letters*, 82(3), 660-663.
- Neiman, A., Schimansky-Geier, L., Cornell-Bell, A., & Moss, F. (1999b). Noise-enhanced phase synchronization in excitable media. *Physical Review Letters*, 83(23), 4896-4899.
- Neiman, A., Schimansky-Geier, Moss, F., Shulgin, B., & Collins, J. J. (1999c). Synchronization of noisy systems by stochastic signals. *Physical Review E*, 60(1), 284-292.
- Neiman, A. and Russell, D. F. (2002). Synchronization of noise-induced bursts in noncoupled sensory neurons. *Physical Review Letters*, 88, 138103.
- Niebur, E. & Koch, C. (1994). A model for the neuronal implementation of selective visual attention based on temporal correlation among neurons. *Journal of Computational Neuroscience*, 1, 141-158.
- O'Craven, K. M., Rosen, B. R., Kwong, K. K., Treisman, A. & Savoy, R. L. (1997). Voluntary attention modulates fMRI activity in human MT-MST. *Neuron*, 18, 591-598.
- O'Shea, R. P., & Crassini, B. (1984). Binocular rivalry occurs without simultaneous presentation of rival stimuli. *Perception & Psychophysics*, 36(3), 266-276.
- Phillips, W. A., & Singer, W. (1997). In search of common foundations for cortical computation. *Behavioral and Brain Sciences*, 20, 657-722.
- Pikovsky, A. S. & Kurths, J. (1997). Coherence Resonance in a Noise-Driven Excitable System. *Physical Review Letters*, 78, 775-778.
- Pikovsky, A., Rosenbaum, M., & Kurths, J. (2003). *Synchronization: A universal concept in nonlinear sciences*. Cambridge University Press, Cambridge.
- Pollen (2002)
- Polonsky, A., Blake, R., Braun, J., & Heeger, D. J. (2000). Neuronal activity in human primary visual cortex correlates with perception during binocular rivalry. *Nature Neuroscience*, 3(11), 1153-1159.
- Posner, M. I., Snyder, C. R., & Davidson, B. J. (1980). Attention and the detection of signals. *Journal of Experimental Psychology*, 109, 160-174.
- Rager, G. & Singer, W. (1998). The response of cat visual cortex to flicker stimuli of variable frequency. *European Journal of Neuroscience*. 10, 1856-1877.
- Regan, D. (1989). *Human brain electrophysiology: Evoked potentials and evoked magnetic fields in science and medicine*. Elsevier, New York.

- Regan, D. & Spekreijse, H. (1986). Evoked potentials in vision research: 1961-1985. *Vision Research*, 26, 1461-1480.
- Reynolds, J. H., Chelazzi, L., & Desimone, R. (1999). Competitive mechanisms subserve attention in macaque areas V2 and V4. *Journal of Neuroscience*, 19, 1736-1735.
- Reynolds, J. H., Pasternak, T. & Desimone, R. (2000). Attention increases sensitivity of V4 neurons. *Neuron*, 26, 703-714.
- Reynolds, J. H. & Chelazzi, L. (2004). Attentional modulation of visual processing. *Annual Review of Neuroscience*, 27, 611-647.
- Riani, M. & Simonotto, E. (1994). Stochastic resonance in the perceptual interpretation of ambiguous figures : A neural network model. *Phys. Rev. Lett.* 72, 3120-3123.
- Richards, W., Wilson, H.R., and Sommer, M.A. (1994). Chaos in percepts? *Biological Cybernetics*, 70, 345-349.
- Rosenblum, M., Pikovsky, A. & Kurths, J. (1996). Phase synchronization of chaotic oscillators. *Physical review letters.* 76, 1804.
- Rosenblum, M., Pikovsky, A. & Kurths, J. (1997). From phase to lag synchronization in coupled chaotic oscillators. *Physical review letters.* 78, 4193-4196.
- Rulkov, N. F., Sushchik, M. M., Tsimring, L. S., & Abarbanel, H. D. I. (1995). Generalized synchronization of chaos in directionally coupled chaotic systems. *Physical review E.* 51(2), 980-994.
- Russell, D. F., Wilkens, L. A. & Moss, F. (1999). Use of stochastic resonance by paddle fish for feeding. *Nature*, 402, 291-294.
- Saalman, Y. B., Pigareve, I. V., & Vidyasagar, T. R. (2007). Neural mechanisms of visual attention: How top-down feedback highlights relevant locations. *Science.* 316, 1612-1615.
- Schiller, P. H., Logothetis, N. K., & Charles, E. R. (1990). Role of the color-opponent and broad-band channels in vision. *Visual Neuroscience*, 5, 321-346.
- Schröder, J.-H., Fries, P., Roelfsema, P. R., & Singer, W., & Engel, A. K. (2002). Ocular dominance in extrastriate cortex of strabismic amblyopic cats. *Vision Research*, 42, 29-39.
- Shapley, R. (1995). Parallel neural pathways and visual function. In M. S. Gazzaniga (Ed.), *The Cognitive Neurosciences* (pp. 315-342). Cambridge, MA: MIT Press.
- Shapley, R. (2004). A new view of the primary visual cortex. *Neural Networks*, 17, 615-623.
- Sheinberg, D. L. & Logothetis, N. K. (1997). The role of temporal cortical areas in perceptual organization. *Proceedings of the National Academy of Sciences USA*, 94, 3408-3413.
- Shulgin, B., Neiman, A., & Anishchenko, V. (1995). Mean switching frequency locking in stochastic bistable systems driven by a periodic force. *Physical Review Letters*, 75(23), 4157-4160.
- Simonotto, E., Riani, M., Seife, C., Roberts, M., Twitty, J. & Moss, F. (1997). Visual perception of stochastic resonance. *Physical Review Letters*, 78, 1186-1189.
- Singer, W. (1999). Striving for coherence. *Nature*, 397(4), 391-393.
- Singer, W. & Gray, C. M. (1995) Visual feature integration and the temporal correlation hypothesis. *Annual Review of Neuroscience*, 18, 555-586.
- Sperling, G. (1970). Binocular vision: A physical and neural theory. *American Journal of Psychology*, 83, 461-534.

- Sperling, G. & Melchner, M. J. (1978). The attention operating characteristic: examples from visual search. *Science*, 202, 315-318.
- Spitzer, H., Desimone, R. & Moran, J. Increased attention enhances both behavioral and neuronal performance. *Science* 240, 338-40 (1988).
- Srinivasan, R., Russell, D. P., Edelman, G. M., & Tononi, G. (1999). Increased synchronization of neuromagnetic responses during conscious perception. *Journal of Neuroscience*, 19(13), 5435-5448.
- Steinmetz, P. N. et al. (2000). Attention modulates synchronized neuronal firing in primate somatosensory cortex. *Nature*, 404, 187-190.
- Strogatz, S. (2003). Sync: The emerging science of spontaneous order. *Hyperion*
- Sugie, N. (1982). Neural models of brightness perception and retinal rivalry in binocular vision. *Biological Cybernetics*, 43, 13-21.
- Suzuki, S. (2001). Attention-dependent brief adaptation to contour orientation: a high-level aftereffect for convexity? *Vision Research*, 41, 3883-3902.
- Suzuki, S. & Grabowecky, M. (2002a). Evidence for perceptual “trapping” and adaptation in multistable binocular rivalry. *Neuron*, 36, 143-157.
- Suzuki, S., & Grabowecky, M. (2002b). Overlapping features can be parsed on the basis of rapid temporal cues that produce stable emergent percepts. *Vision Research*, 42, 2669-2692.
- Suzuki, S. & Grabowecky, M. (2004). Long-term speeding of alternations in binocular rivalry: potential mediation by primary visual cortex. *Annual meeting of the Vision Sciences Society*, Sarasota, FL, U.S.A.
- Tallon-Baudry, C., Bertrand, O., Delpuech, C., & Premier, J. (1996). Stimulus specificity of phase-locked and non-phase-locked 40 Hz visual responses in human. *Journal of Neuroscience*, 16, 4240-4249.
- Taylor, M.M., and Aldridge, K.D. (1974). Stochastic processes in reversing figure perception. *Perception & Psychophysics*, 16, 9-27.
- Tong, F. & Engel, S. A. (2001). Interocular rivalry revealed in the human cortical blind-spot representation. *Nature*, 411, 195-199.
- Tononi, G., Srinivasan, R., Russell, D. P., & Edelman, G. M. (1998). Investigating neural correlates of conscious perception by frequency-tagged neuromagnetic responses. *Proceedings of the National Academy of Sciences USA*, 95, 3198-3203.
- Treisman, A. & Sato. S. (1990). Conjunction search revisited. *Journal of Experimental Psychology: Human Perception and Performance*, 16, 459-478.
- Ungerleider, L. G. & Mishkin, M. (1982). Two cortical visual systems. In D. J. Ingle, M. A. Goodale, and R. J. W. Mansfield (Eds.), *Analysis of Visual Behavior* (pp. 549-586). Cambridge, MA: MIT Press.
- Vanni, S., Warnking, J., Dojat, M., Delon-Martin, C., Bullier, J., & Segebarth, C. (2004). Sequence of pattern onset responses in the human visual areas: an fMRI constrained VEP source analysis. *NeuroImage*, 21, 801-817.
- Varela, F., Lachaux, J-P., Rodriguez, E., & Martinerie, J. (2001). The brainweb: phase synchronization and large-scale integration. *Nature Reviews Neuroscience*. 2, 229-239.
- Wade, N. J. (1974). The effect of orientation in binocular contour rivalry of real images and afterimages. *Perception & Psychophysics*, 15(2), 227-232.
- Ward, L. (2002). *Dynamical Cognitive Science*, MIT Press: Cambridge, MA.

- Ward, L. M. (2003). Synchronous neural oscillations and cognitive processes. *Trends in Cognitive Sciences*, 7(12), 553-559.
- Wiesenfeld, K. & Moss, F. (1995). Stochastic resonance and the benefits of noise: from ice ages to crayfish and SQUIDS. *Nature*, 373, 33-36.
- Williford, T. & Maunsell, J. H. (2006). Effects of spatial attention on contrast response functions in macaque area V4. *Journal of Neurophysiology*, 96, 40-54.
- Wilson, H. R. (1999). *Spikes, decisions and actions: The dynamical foundations of neuroscience*. Oxford University Press, (p. 131-134).
- Wilson, H. R. (2003). Computational evidence for a rivalry hierarchy in vision. *Proceedings of the National Academy of Sciences USA*, 100(24), 14499-14503.
- Wilson, H. R., Krupa, B., & Wilkinson, F. (2000). Dynamics of perceptual oscillations in form vision. *Nature Neuroscience*, 3(2), 170-176.
- Wilson, H. R. Blake, R., & Lee, S-H. (2001). Dynamics of traveling waves in visual perception. *Nature*, 412, 907-910.
- Wolfe, J. M. (1984). Reversing ocular dominance and suppression in a single flash. *Vision Research*, 24, 471-478.
- Womelsdorf, T., Schoffelen, J-M., Oostenveld, R., Singer, W., Desimone, R., Engel, A. K., & Fries, P. (2007). Modulation of neuronal interactions through neuronal synchronization. *Science*. 316, 1609-1612.
- Yoshikawa, T., Levitt, J. B., & Lund, J. S. (1994). Independence and merger of thalamocortical channels within macaque monkey primary visual cortex: anatomy of interlaminar projections. *Visual Neuroscience*, 11, 467-489.

## FIGURES

Figure 1

Motion of a particle in a double-well potential. Noise induces irregular transitions between two stable states (dashed line). A symmetric bistable potential is periodically rocked by a weak signal. The presence of an optimal amount of noise (so that the average stochastic escape time approximately matches half the period of the signal) will statistically induce synchronized hopping events between the two locally stable states.

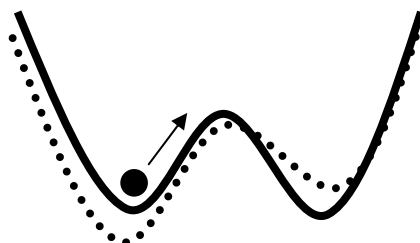


Figure 1-1

The contrast-, response-, and activity-gain hypotheses regarding how voluntary visual spatial attention boosts neural responses. A. According to the contrast-gain hypothesis, attention increases the effective contrast of attended stimuli, shifting the contrast response function to the left. B. According to the response- and activity-gain hypotheses, attention multiplicatively increases neural responses to attended stimuli, either with (activity gain) or without (response gain) attention effects on spontaneous neural activity. The upper panels show hypothetical contrast-response functions for attended and ignored conditions, and the bottom panels show the difference between attended and ignored contrast-response functions.

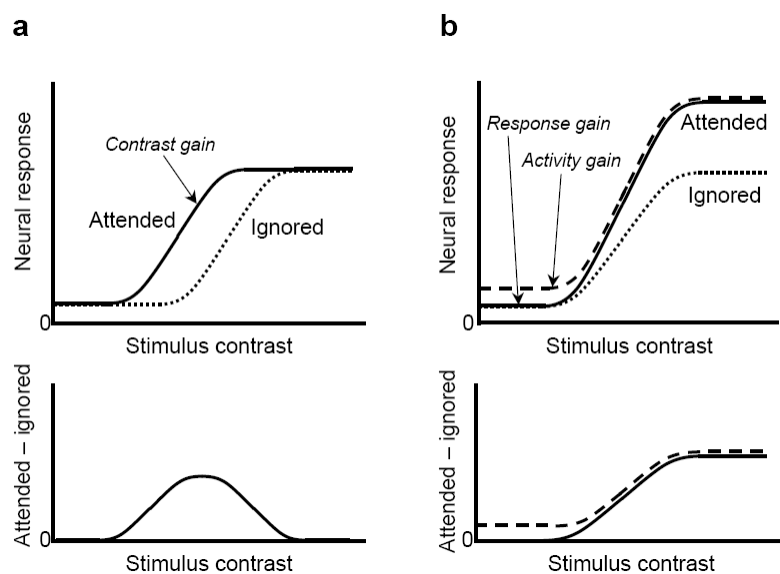


Figure 1-2

Stimuli and a trial sequence. A. Two circular gratings were presented in opposite hemifields. Both gratings were flickered (one at 12.50 Hz and the other at 16.67 Hz) between a dark phase and a light phase; for illustration, the dark phase is shown on the left and the light phase is shown on the right. B. Each trial was initiated by a button press, followed by a central arrow (attention cue) indicating the grating to be attended, a fixation screen, and then a 4.8-s presentation of the flickered gratings.

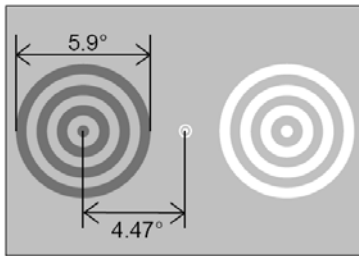
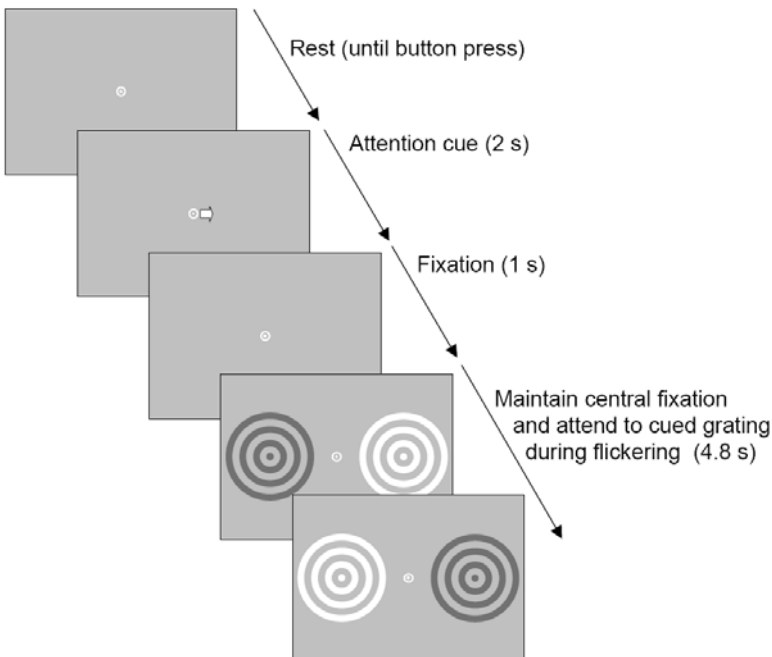
**a****b**

Figure 1-3

Topographic plots of 2<sup>nd</sup> harmonic of the standardized SSVEPs to the 16.67-Hz grating (A) and the 12.50-Hz grating (B), averaged across observers and stimulus contrasts. Color-scale data were interpolated based on a fine Cartesian grid. Positive and negative values indicate responses above and below the mean level, respectively, in  $z$  units. The left column shows SSVEP topographies when the relevant grating was presented to the right visual field, whereas the right column shows SSVEP topographies when the relevant grating was presented to the left visual field. Separate rows show conditions in which the relevant grating was attended (upper row), the relevant grating was ignored (middle row), or show the difference between attended and ignored conditions (lower row). Maximal responses and maximal attention effects at contralateral posterior locations are apparent in all cases.

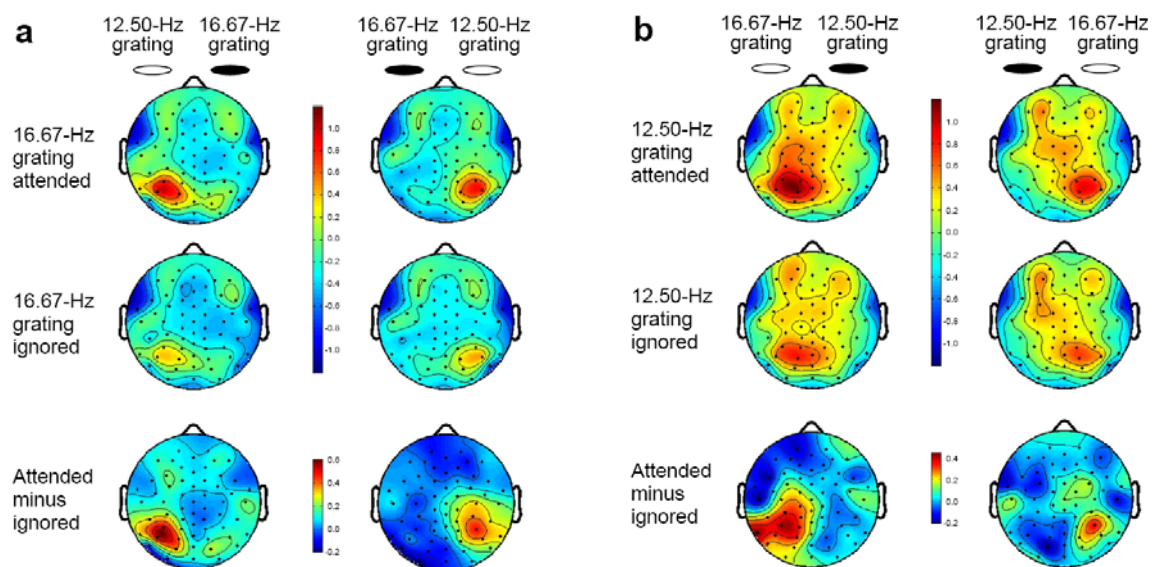


Figure 1-4  
 SSVEP contrast-response functions for the 16.67-Hz grating (B) and the 12.50-Hz grating (C), computed from the 10 scalp electrodes (illustrated in A) from which strong stimulus responses and attention effects were obtained (see Figure 1-3). Contralateral responses are shown on the left and ipsilateral responses are shown on the right. Contrast-response functions obtained when the relevant grating was attended are shown in red solid lines. Contrast-response functions obtained when the relevant grating was ignored are shown in blue dotted lines. For the contralateral responses, contrast dependencies of the attention effects (i.e., attended minus ignored conditions) are shown in the insets. The continuous curves indicate fits based on the Naka-Rushton equation; for the 16.67-Hz grating,  $r^2$  for the fits are 0.995 (contralateral attended), 0.991 (contralateral ignored), 0.982 (ipsilateral attended), and 0.956 (ipsilateral ignored); for the 12.50-Hz grating, the corresponding  $r^2$  are 0.994, 0.987, 0.975 and 0.992. The error bars indicate  $\pm 1$  SEM.

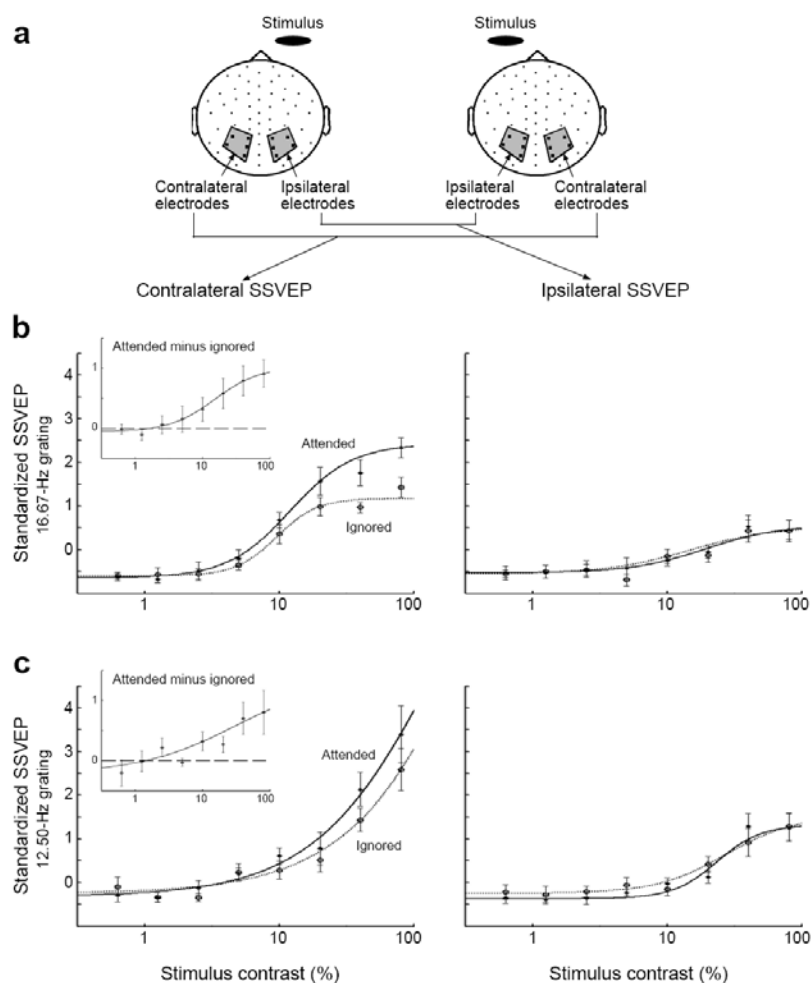


Figure 1-5

Representative simulation results showing that averaging neuronal attentional contrast-gain effects over a population of neurons with a range of contrast-response functions and attentional contrast-gain magnitudes produces contrast gain. This indicates that attentional response gain cannot emerge at the population level from averaging attentional contrast-gain effects on individual neurons. The average attention effect (i.e., the average attended contrast-response function minus the average ignored contrast-response function) is plotted for each simulated neural population ( $N = 1000$ ) with a distribution of neuronal contrast-response functions and attentional contrast-gain magnitudes. To clearly show the shape of each attention-effect curve, the values are normalized relative to the peak value. The 48 representative attention-effect curves shown are based on even sampling of population parameter statistics from the following ranges. Because neurons in higher visual areas tend to saturate at lower contrasts (see Suzuki 2001 for a review), mean  $C_{50}$  was sampled between 0.43 (a published value for V1 (Geisler & Albrecht, 1997)) and zero, while its standard deviation was fixed at 0.31 (a published value for V1 (Geisler & Albrecht, 1997)). Mean neuronal attentional contrast gain (i.e., mean percentage reduction in  $C_{50}$  due to attention) was sampled between 0% (no attention effect) and 100% (maximal attention effect), while its standard deviation was sampled between 0% and 200%. The mean and standard deviation for the parameter  $n$  were 2.5 and 1.4 (published values for V1 (Geisler & Albrecht, 1997)), those for  $b$  were 0.1 and 0.2;  $a$  was set to unity. See text and Eq. 1-1 for explanation of these parameters. Simulation results still showed peaked attention-effect curves consistent with contrast gain when we sampled from wider ranges of means and standard deviations for the parameter values including the values reported for V4 neurons (Williford & Maunsell, 2006).

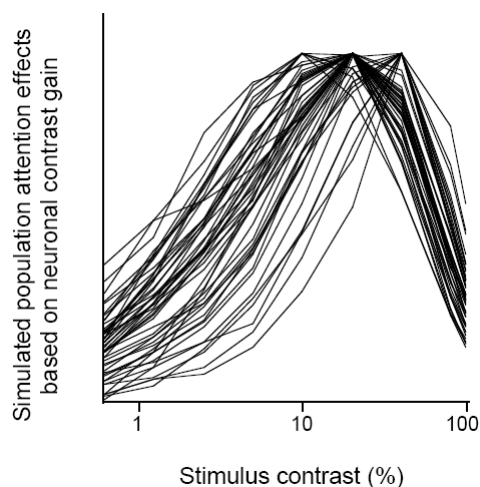


Figure 1-6

ITPC for second-harmonic SSVEPs averaged across contralateral focal electrodes, which are illustrated in Figure 4a. (a) Time-averaged ITPCs (averaged over the entire trial period) when gratings were attended versus ignored. ITPCs are shown separately for the two flicker frequencies (16.67-Hz and 12.50-Hz) and for the two highest contrasts (40% and 80%).

Attention significantly increased ITPC in all conditions;  $t_7 = 2.758$ ,  $P < 0.03$  and  $t_7 = 2.409$ ,  $P < 0.05$  for 40% and 80% contrasts, respectively, for the 16.67-Hz flickered grating, and  $t_7 = 3.608$ ,  $P < 0.01$  and  $t_7 = 2.878$ ,  $P < 0.03$  for 40% and 80% contrasts, respectively, for the 12.50-Hz grating. (b) Time course of ITPCs when gratings were attended versus ignored. ITPCs (averaged across 40% and 80% contrasts) are shown separately for the 16.67-Hz grating (upper) and the 12.50-Hz grating (lower). Time zero corresponds to the grating onset. Note that it takes a few hundred milliseconds for the effects of attention on synchronization to emerge after the grating onset. The data have been averaged across observers and the error bars shown in a indicate  $\pm 1$  s.e.m., with individual variability in baseline ITPC removed.

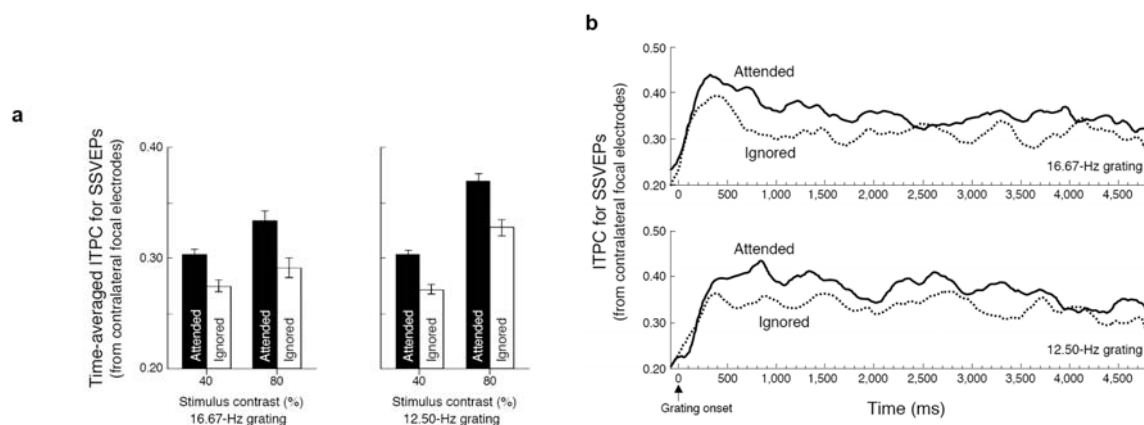


Figure 1-7

Contrast dependence of inter-trial phase coherence (ITPC) for SSVEPs (averaged across contralateral focal electrodes, see Figure 1-4A) when gratings were attended (solid lines) and ignored (dashed lines). Top. ITPC contrast-dependence functions (averaged across 16.67-Hz and 12.50-Hz gratings) averaged from 50 to 4800 ms. Bottom. ITPC contrast-dependence functions shown separately for different time periods during sustained attention. The continuous curves indicate fits based on the Naka-Rushton equation;  $r^2$  for the fits are 0.991 (attended) and 0.987 (ignored) for the 50-4800 ms period (red), 0.692 (attended) and 0.933 (ignored) for the 50-200 ms period (black), 0.946 (attended) and 0.951 (ignored) for the 200-400 ms period (orange), 0.985 (attended) and 0.967 (ignored) for the 400-1000 ms period (purple), and 0.994 (attended) and 0.985 (ignored) for the 1000-4800 ms period (green). Note that, except for the earliest interval that shows no attention effect, ITPC contrast-dependence functions for all other periods show a response-gain-type profile.

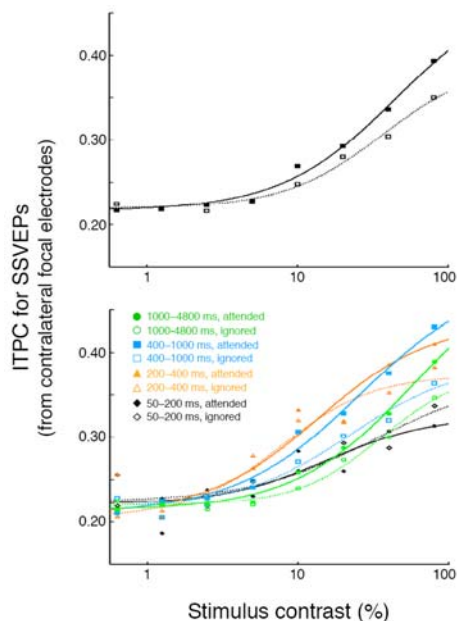


Figure 1-8

Examples of probe displays for the control experiment. A target-present display is shown in A (the target is the pair of identically oriented oblique lines at the location of the left grating). A target-absent display (oblique lines are differently oriented within each pair) is shown in B. Vertical distractors were added so that grouping did not create an easily detectable emergent feature.

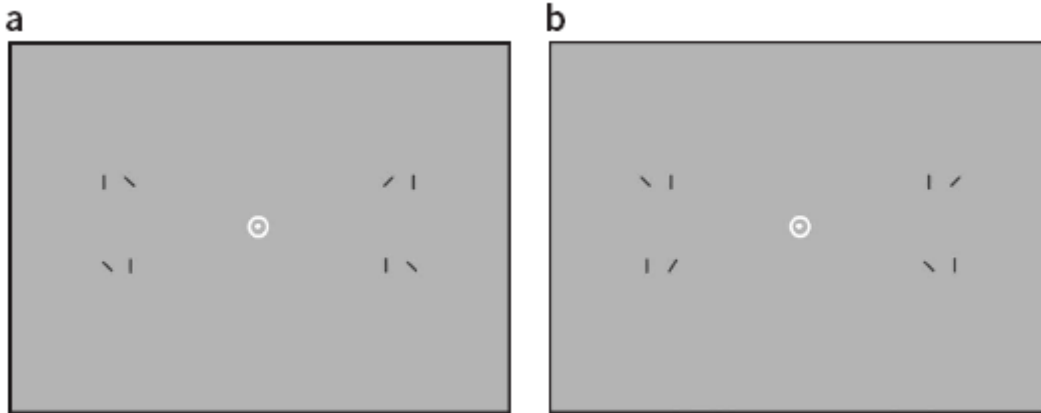


Figure 2-1

Stimuli and a trial sequence. On each trial, a circular grating was presented in either the left or right visual hemifield. The grating was flickered between a light phase and a dark phase at various frequencies (6.25, 8.33, 12.5, 16.7, and 25 Hz). Each trial was initiated by a button press, followed by a fixation screen, and then a 4.8-sec presentation of the flickered grating.

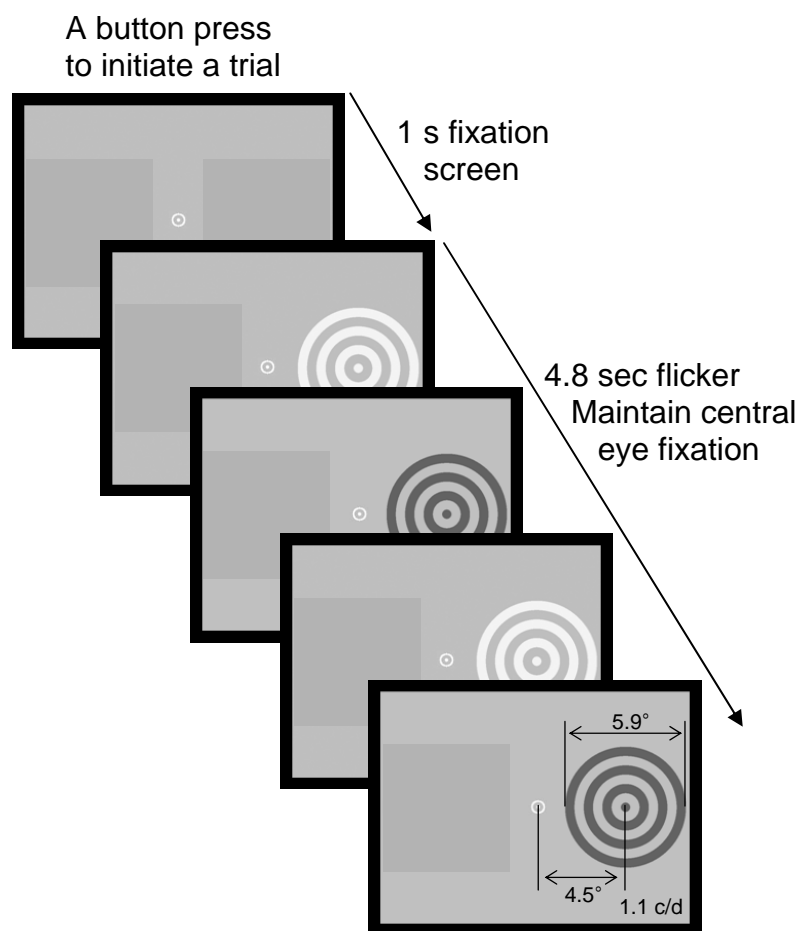


Figure 2-2

A. Topographic plots of the 1<sup>st</sup> (upper row) and 2<sup>nd</sup> (lower row) harmonics of the standardized SSVEPs elicited by the flickered grating, averaged across observers and flicker frequencies. Color-scale data were interpolated based on a fine Cartesian grid. Positive and negative values indicate responses above and below the mean level, respectively, in  $z$  units. The left column shows SSVEP topographies when the grating was presented to the right visual hemifield, and the right column shows SSVEP topographies when the grating was presented to the left visual hemifield. B. Contralateral (gray bars) and ipsilateral (white bars) SSVEPs for the 1<sup>st</sup> and 2<sup>nd</sup> harmonics averaged from the 10 illustrated posterior scalp electrodes from which strong SSVEPs were obtained (see A). The graphs confirm that the 1<sup>st</sup> harmonic was medial (non-lateralized) whereas the 2<sup>nd</sup> harmonic was strongly contralateral. C. The degree of lateralization (contralateral minus ipsilateral standardized SSVEPs) for the 1<sup>st</sup> (dashed curve) and 2<sup>nd</sup> (solid

curve) harmonics as a function of the flicker frequency. The numbers within the plot represent the corresponding response frequencies (the same as the flicker frequencies for the 1<sup>st</sup> harmonic and doubled for the 2<sup>nd</sup> harmonic). The asterisks indicate statistically significant lateralization (i.e., significant deviations from zero) at  $P < 0.05$ . D. The contralateral (solid line) and ipsilateral (dashed line) standardized SSVEPs for the 1<sup>st</sup> (left panel) and 2<sup>nd</sup> (right panel) harmonics. All error bars represent  $\pm 1$  SEM with the variance due to the overall differences across observers removed.

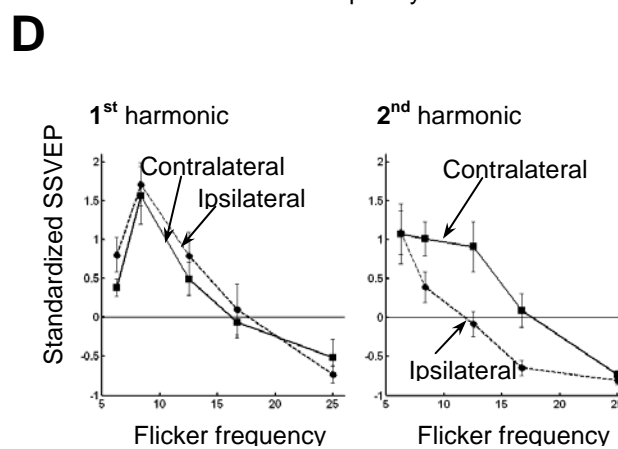
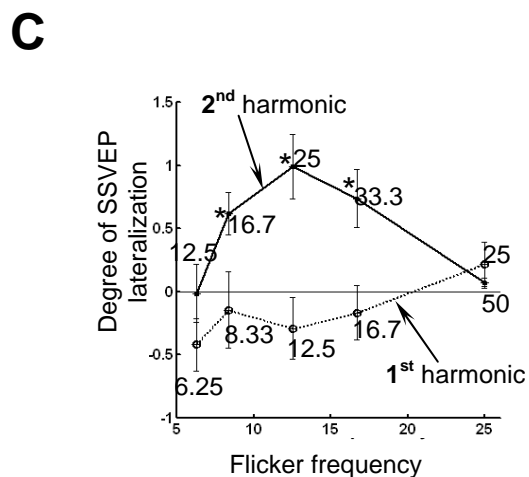
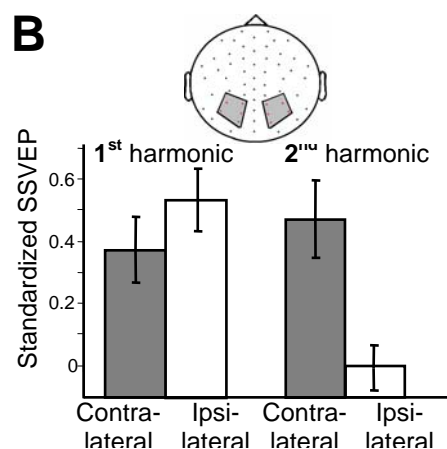
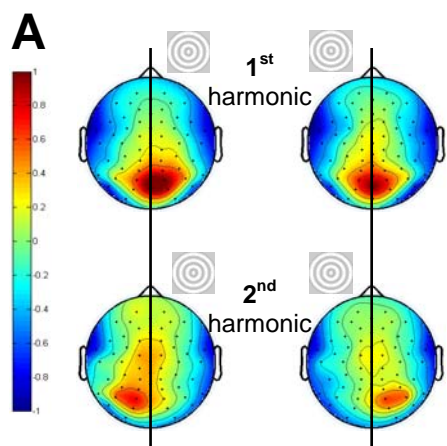


Figure 2-3

Stimuli and a trial sequence (adapted from Kim *et al.*, 2007). On each trial two circular gratings were presented in opposite hemifields. Gratings were flickered (between a light and dark phase) at different frequencies, one at 12.50 Hz and the other at 16.67 Hz. Each trial was initiated by a button press, followed by a central arrow indicating the grating to be attended, a fixation screen, and then a 4.8-s presentation of the flickered gratings.

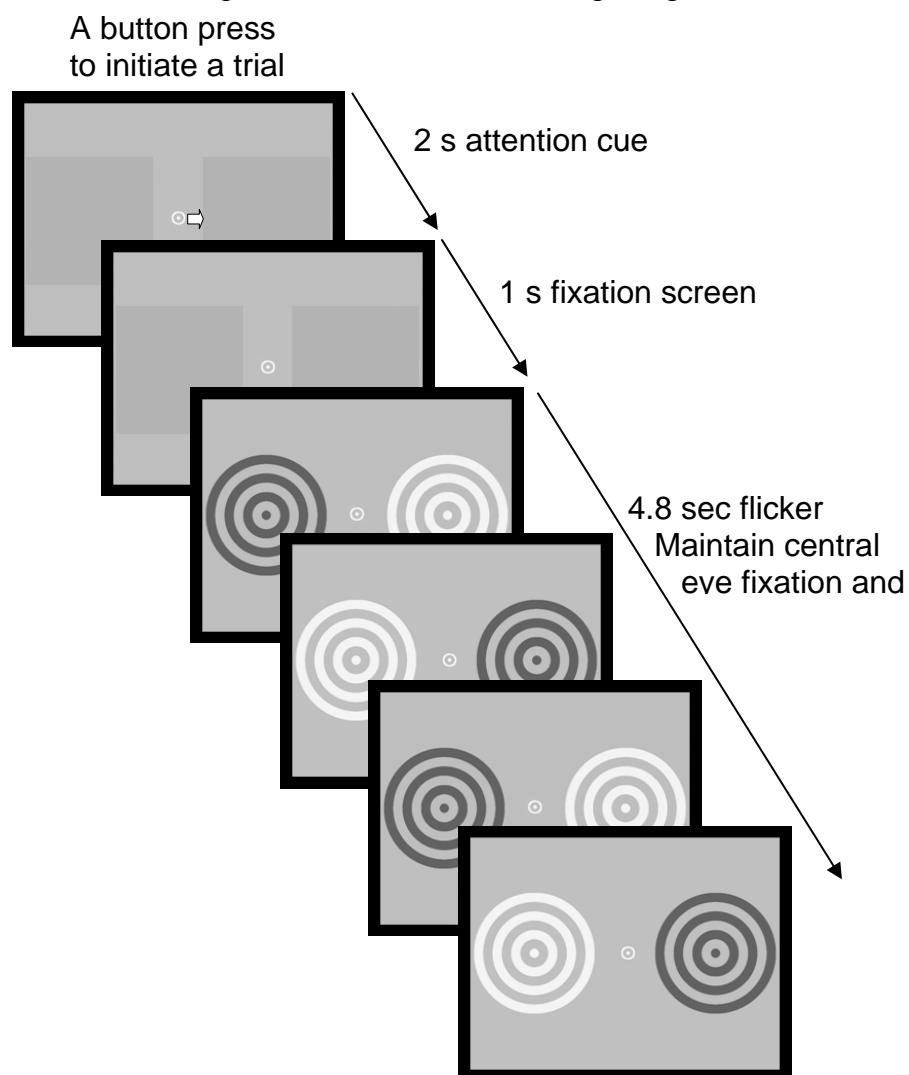


Figure 2-4

Topographic plots of the 1<sup>st</sup> harmonic (upper row) and the 2<sup>nd</sup> harmonic (lower row) of the standardized SSVEPs elicited by the gratings presented in the left or right visual hemifield (indicated by the circle around the grating icon), averaged across observers, grating contrast, flicker frequencies, and attention conditions (i.e., attended or ignored). Color-scale data were interpolated based on a fine Cartesian grid. Positive and negative values indicate responses above and below the mean level, respectively, in  $z$  units. The left column shows SSVEP topographies

elicited by the gratings presented in the right visual hemifield, whereas the right column shows SSVEP topographies elicited by the gratings presented in the left visual hemifield. B. Upper panel. The 1<sup>st</sup> and 2<sup>nd</sup> harmonics of the standardized SSVEPs elicited by the attended and ignored gratings, averaged across observers, grating contrast, and flicker frequencies. The 1<sup>st</sup> and 2<sup>nd</sup> harmonics were averaged from the posterior scalp electrodes based on their characteristic topographies (see A); the 1<sup>st</sup> harmonic was averaged from the five central posterior scalp electrodes, whereas the 2<sup>nd</sup> harmonic was averaged from the five contralateral posterior scalp electrodes (see the illustration). Attention modulated the 2<sup>nd</sup> harmonic but not the 1<sup>st</sup> harmonic. Lower panels. The contrast response functions (i.e., standardized SSVEPs as a function of stimulus contrast) for the 1<sup>st</sup> harmonic (left panel) and 2<sup>nd</sup> harmonic (right panel) elicited by the attended and ignored gratings. All error bars represent  $\pm 1$  SEM with the variance due to the overall differences across observers removed.

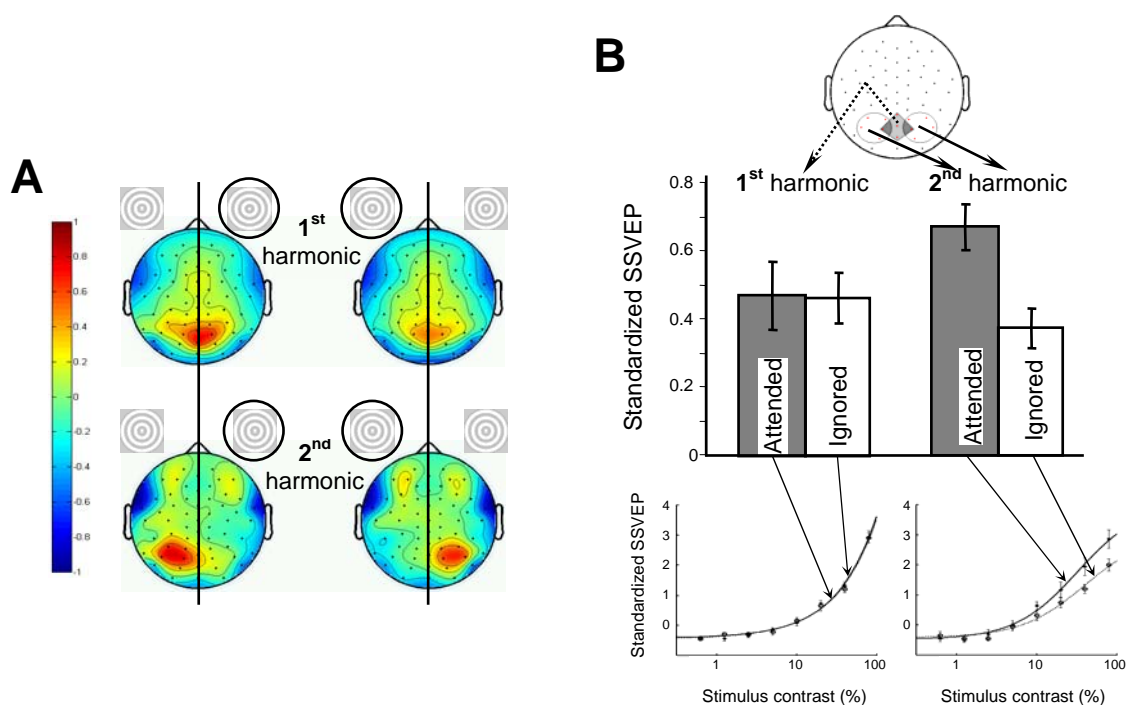


Figure 3-1

A cartoon illustration of a double-well potential framework describing binocular rivalry under periodic contrast modulations. The left and right wells correspond to representations of the “+” and “x” shapes, respectively. The depths of the two wells were periodically modulated in opposite phase by modulating the luminance contrasts of the two images in opposite phase (see text for details). The position of the smiley face represents the perceptual state (i.e., the perceived shape). If the neural mechanisms underlying the double-well potential landscape interacted appropriately with noise to produce stochastic resonance under appropriate conditions, the dominance-duration distribution should show resonance peaks at (A) one times the contrast-modulation half-period, HP, (B) three times the modulation half-period, 3 HP, and at other odd-integer multiples of the modulation half-period.

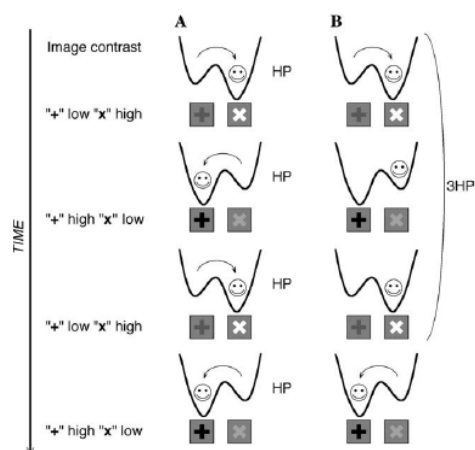


Figure 3-2

The stimuli used to induce binocular rivalry. The two images were presented dichoptically using a four-mirror stereoscope. The high-contrast textured frames were binocularly presented around the rivaling shapes to facilitate stable binocular alignment. Perception spontaneously alternated between “+” and “x” shapes. To induce stochastic resonance, the luminance contrasts of the two shapes were temporally modulated in opposite phase at various frequencies. A non-rivaling grating was presented binocularly on the right side (as shown in the figure) to balance the overall stimulus configuration and help stabilize fixation (the grating was not presented in the blink-allowed condition).

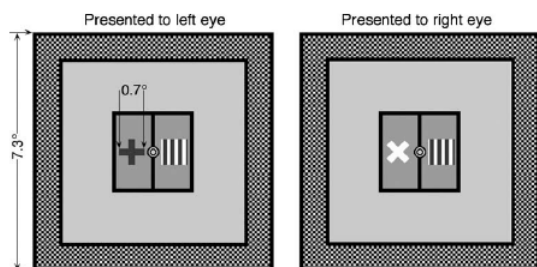




Figure 3-4

$P_1$  amplitude and gain due to periodic contrast-modulation signals. Upper panels:  $P_1$  amplitude for the dominance-duration distributions as a function of the contrast-modulation frequency (solid curve), and the corresponding area proportions for the control distributions (dashed curve). Lower panels:  $P_1$  gain computed as the difference between the solid and dashed curves from the upper panels. (A) Observer SS, 0.25 baseline contrast with no blinking. (B) Observer YS, 0.50 baseline contrast with blinking allowed. (C) Observer YS, 0.50 baseline contrast with no blinking. (D) Observer ET, 0.50 baseline contrast with no blinking. The primary graphs show the results with contrast-modulation amplitudes of 30% (A, C, and D) and 40% (B). The inset graphs (A and C) show the results with 20% contrast modulations. For all observers, the results with other baseline contrasts were similar.

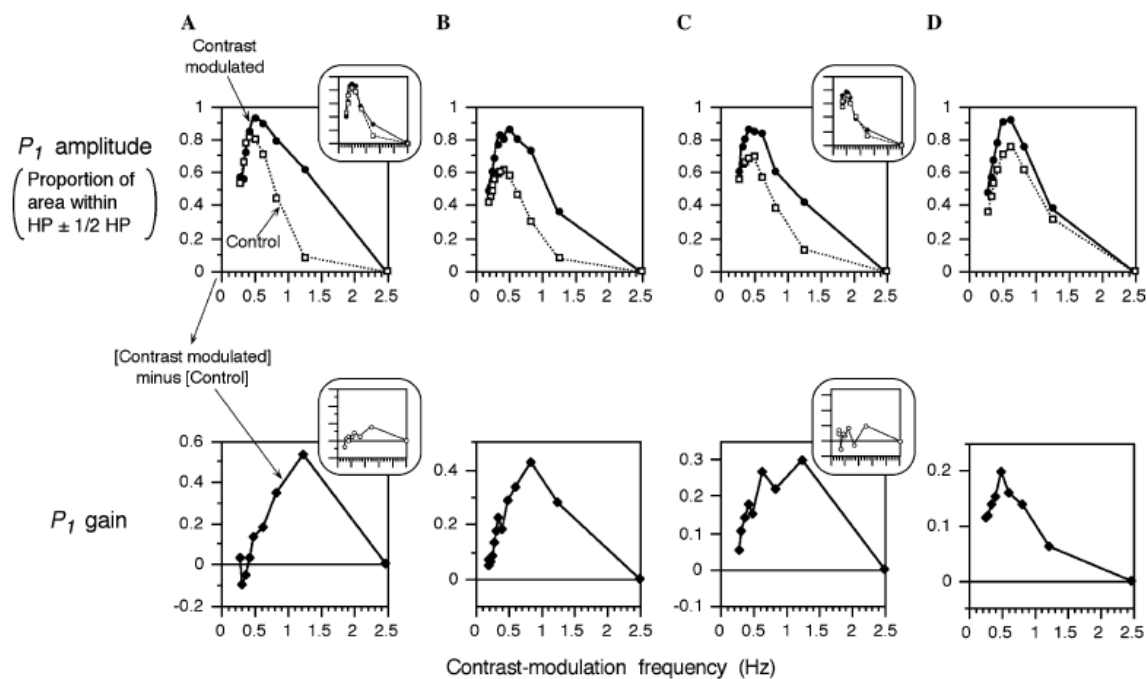


Figure 3-5

Coefficient of variation (CV = standard deviation/mean) as a function of the contrast-modulation frequency (Hz). The data (the no-blink conditions only) are shown for the baseline contrasts of 0.50 (left panels) and 0.25 (right panels) for each observer. The gray bands represent the average spontaneous alternation rates (the lower and upper bounds derived from the mean and median dominance durations, respectively). The primary graphs show the results with 30% contrast modulations. The inset graphs (for observers SS and YS) show the results with 20% contrast modulations.

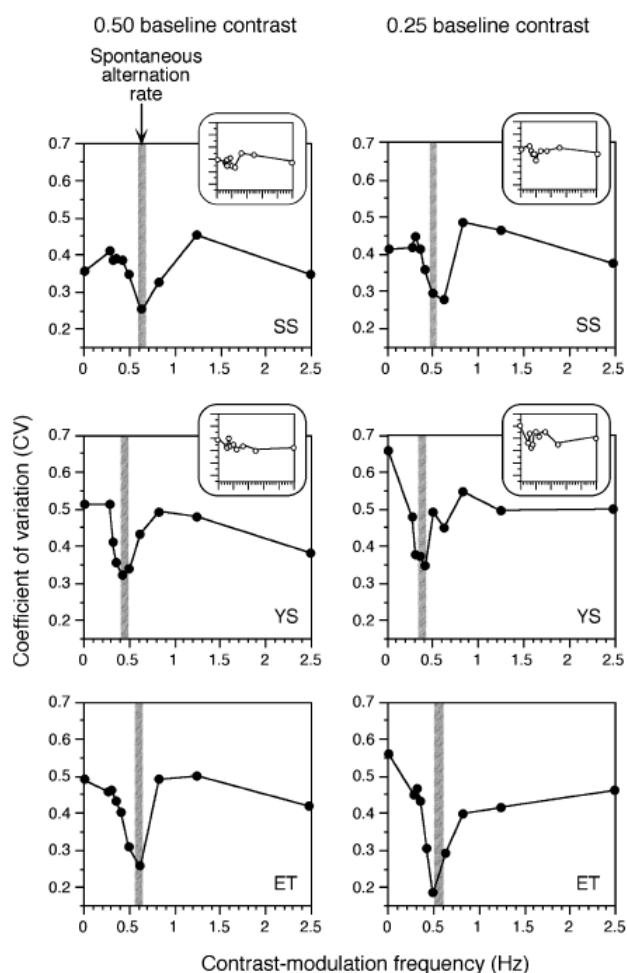


Figure 3-6

The relationship between the resonance frequency (the contrast-modulation frequency that minimizes CV) and the mean spontaneous alternation rate. A positive correlation is apparent ( $r^2 = 0.735$ ). Furthermore, the data points lie close to the diagonal (with slope = 1), indicating that the resonance frequency closely followed the average spontaneous alternation rate while the latter varied due to individual differences, the use of different baseline contrasts (0.25 or 0.50), and the within-trial slowing of binocular rivalry. Connected pairs of symbols represent the first

half-trials (upper right) and the second half-trials (lower left) for each baseline contrast for each observer.

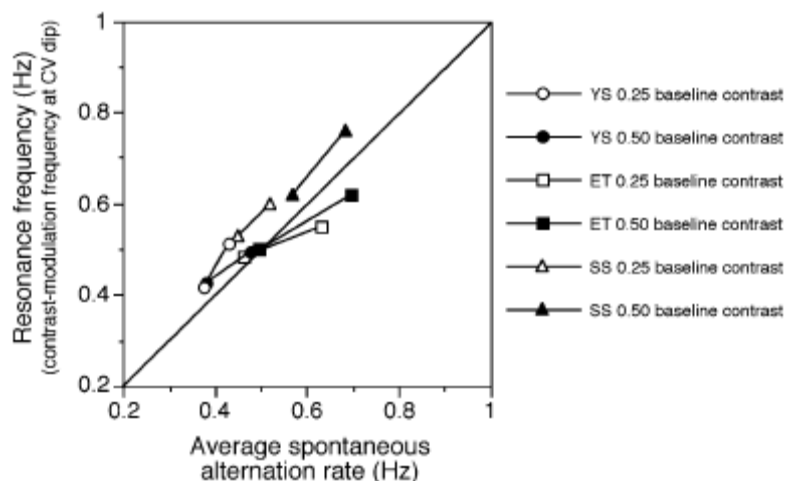


Figure 3-7

Fitting the dominance-duration distributions for contrast-modulation frequencies from 0.28 to 2.48 Hz (with the corresponding half-periods [HP] from 1800 to 200 ms), using the astable multivibrator model based on a Schmitt trigger (known to exhibit stochastic resonance). The thin curves show the data and the thick curves show the fits. Note that the locations of the peaks at the odd-integer multiples of the modulation half-period (indicated by the vertical lines), the number of the peaks, and the relative amplitude of the peaks are simulated reasonably well. Observer YS's data for 0.50 baseline contrast (blinking allowed) are shown as an example. The fits to other data are similar.

